

https://dspace.org/

Adsorption studies on supported gold catalysts using temperature programmed desorption (TPD)

Linganiso, Linda, Zikhona

2007-06
Wits University
http://hdl.handle.net/10539/20167

Downloaded from a DSpace repository. https://dspace.org/

ADSORPTION STUDIES ON SUPPORTED GOLD CATALYSTS USING TEMPERATURE PROGRAMMED DESORPTION (TPD)

by

LINDA ZIKHONA LINGANISO

Submitted in fulfilment of the requirements for the degree of

Masters of Science in the Faculty of Science

Department of Chemistry

University of the Witwatersrand

Private / Bag X 3

Wits

2050

Johannesburg

South Africa

June 2007

SUPERVISER: PROF. M. S. SCURRELL

DEDICATED TO MY MOTHER VUYOKAZI

DECLARATION

I hereby declare that adsorption studies on supported gold catalysts using temperature-programmed desorption is my own work and is submitted to the University of the Witwatersrand for the degree of Masters of Science and has not been previously submitted for any other degree in any other university and all the material contained therein has been acknowledged.



.....

LINGANISO LINDA ZIKHONA

AKNOWLEDGEMENTS

I would like to express my deepest appreciation to the following people:

My supervisor Prof. Mike Scurrell for his advice, guidance and support throughout this project. I would like to thank him for his encouragement, patience, and the ability he has to instruct me during hard times of this project.

My friend Walter Ngobeni for his valuable assistance, inputs and fruitful discussions we have had together.

Also acknowledged is Kaushik Mallick for all the inputs he has given towards this dissertation.

NRF, Canon Colin's Educational Trust of South Africa and Catalysis group for financial assistance.

Special thanks to the University of the Witwatersrand, department of Chemistry for letting me do this research. I would like to thank the Chemistry staff members and the fellow post graduates for being useful, kind and for creating extremely nice environment to work.

I also owe special thanks to my family for the support they always give me throughout my studies.

Finally, I thank God for being my source of strength.

LIST OF ABBREVIATIONS

AES	Auger Electron Spectroscopy
BE	Binding Energy
CVD	Chemical Vapour deposition
CP	Co-precipitation
DBFC	Direct Borohydride Fuel Cell
DP	Deposition-precipitation
E_d	Activation energy of desorption
EXAFS	Extended X-ray Absorption Fine Structure
FCC	Face Centred Cubic
FDS	Flash Desorption Spectroscopy
FID	Flame ionization detector
GC	Gas chromatography
HC's	Hydrocarbons
hr.	Hour
HTR	High Temperature Reduction
IMF	International Monetary Fund
IW	Incipient wetness
LTC	Low temperature calcination
mV	Millivolts
Min.	Minutes
nm	Nanometer
PGMs	Platinum group metals

Pd/C	Carbon supported palladium catalyst
Pd/AuC	Carbon supported palladium-gold catalyst
RT	Room temperature
SAXS	Small-Angle X-ray Scattering
STM	Scanning Tunnelling Microscopy
TCD	Thermal conductivity detector
TEM	Transmission electron microscopy
Temp.	Temperature
TPD	Temperature-Programmed Desorption
TPO	Temperature-Programmed Oxidation
TPR	Temperature-Programmed Reduction
TPSR	Temperature-Programmed Surface Reduction
UHV	Ultra High Vacuum
UV	Ultra Violet
VAM	Vinyl Acetate Monomer
WAXS	Wide-angle x-ray scattering
XANES	X-ray absorption near-edge spectroscopy
XPS	X-ray photoelectron spectroscopy

TABLE OF CONTENTS

DECLARATION.....iii

ACKNOWLEDGEMENTS.....iv

LIST OF ABBREVIATIONS.....v

TABLE OF CONTENTS.....vii

SUMMARY.....xi

CHAPTER 1..... **1**

INTRODUCTION..... **1**

1.1 CATALYSIS..... 1

1.2 WHEN GOLD IS USED AS A CATALYST..... 3

1.3 CHARACTERISTICS OF GOLD AND ITS USES..... 5

1.4 CRYSTAL STRUCTURE AND MORPHOLOGY..... 7

1.5 ROLE OF GOLD IN ENVIRONMENTAL CATALYSIS.. 8

1.5.1 BACKGROUND.....8

1.5.2 WAYS OF CONTROLLING THREE POLLUTANTS (NO_x, CO and HC's.....10

1.5.2.1 EARLY NO_x CONTROL SYSTEMS.....10

1.5.2.2 DEVELOPMENT OF THREE-WAY CATALYSTS.....11

1.6 REFERENCES..... 12

CHAPTER 2..... **15**

TITANIUM DIOXIDE (TiO_2)..... **15**

2.1 STRUCTURE, PROPERTIES AND USES..... 15

2.2 DEGUSSA P25..... 18

2.3 PHASE TRANSFORMATION..... 19

2.4 WHEN TITANIA IS USED AS THE CATALYST SUPPORT..... 21

2.5 REFERENCES..... 24

CHAPTER 3..... **27**

PREPARATION OF SUPPORTED GOLD CATALYST..... 27
3.1 METHODS OF PREPARING SUPPORTED GOLD CATALYSTS..... 27
3.1.1 DEPOSITION-PRECIPITATION METHOD..... 28
3.1.2 IMPREGNATION..... 30
3.1.3 PRECIPITATION..... 31
3.1.4 ION EXCHANGE AND PREPARATION OF GOLD / ZEOLITE CATALYSTS..... 31
3.1.5 VAPOUR-PHASE DEPOSITION AND GRAFTING..... 31
3.1.6 CO-SPUTTERING..... 32
3.1.7 COLLOIDAL MIXING METHOD..... 32
3.2 REFERENCES..... 34
CHAPTER 4..... 36
TEMPERATURE-PROGRAMMED ANALYSIS (TPD)..... 36
4.1 BACKGROUND..... 36
4.2 APPLICATION..... 37
4.2.1 BACKGROUND..... 37
4.2.2 USES OF TPD AGAINST THE ENVIRONMENTAL POLLUTANTS..... 38
4.4 EXPERIMRNTAL TECHNIQUES..... 40
4.4.1 PROCEDURE..... 40
4.5 THEORY..... 41
4.6 TEMPERATURE-PROGRAMMED DESORPTION (TPD)..... 42
4.6.1 BRIEF DESCRIPTION OF THE TECHNIQUE..... 42
4.7 ANALYSIS TECHNIQUES..... 43
4.8 THE NATURE OF GAS SORPTION AT THE SURFACE..... 44
4.9 FUNDAMENTAL PRINCIPLES..... 44
4.9.1 PHYSISORPTION AND CHEMISORPTION..... 44
4.10 THE PROCESS OF GAS ADSORPTION ON THE SURFACE OF SOLID MATERIAL..... 45
4.11 METHANATION..... 45
4.12 REFERENCES..... 46

CHAPTER 5..... 47

EXPERIMENTAL..... 47

5.1 PREPARATION OF THE CATALYST..... 47

5.2 REAGENTS..... 48

5.3 METHOD OF ANALYSIS..... 49

5.3.1 CHARACTERIZATION OF THE CATALYST..... 49

5.3.1.1 Temperature-Programmed Desorption (TPD) apparatus..... 49

5.3.1.2 Powder X-Ray Diffraction (PXRD)..... 52

5.4 REFERENCES.....52

CHAPTER 6.....53

6.1 MOTIVATION FOR THE STUDY..... 53

6.2 OVERALL AIM AND OBJECTIVES..... 53

6.3 REFERENCES..... 53

CHAPTER 7..... 54

RESULTS AND DISCUSSION..... 54

7.1 ADSORPTION OF CARBON MONOXIDE ON TiO_2 OR Au/TiO_2.....55

7.1.1 EFFECT OF GOLD ON SURFACE HETEROGENEITY.....55

7.1.2 EFFECT OF ADSORPTION TEMPERATURE ON Au/TiO_2.....57

7.2 ADSORPTION OF CARBON DIOXIDE ON TiO_2 OR Au/TiO_2.....59

7.2.1 CARBON DIOXIDE ADSORPTION ON TiO_2.. 59

7.2.2 CARBON DIOXIDE ADSORPTION ON Au/TiO_2.....60

7.3 METHANATION..... 62

7.3.1 ADSORPTION OF CO ON Au/TiO_2 OR TiO_2.....62

7.3.1.1 Adsorption of CO on Au/TiO_2 when the methanator is bypassed.....62

7.3.1.2 Adsorption of carbon monoxide on TiO_2..... 63

7.3.1.3 Adsorption of CO on TiO_2 or Au/TiO_2..... 65

7.3.1.4 Adsorption of CO on 1wt% Au/TiO_2 at room temperature..... 66

7.3.1.5 Adsorption of CO on 1wt% Au/TiO_2 at -80°C..... 68

7.3.1.6 Effect of heating rate..... 70
7.3.1.7 Effect of the flow rate..... 72
7.3.1.8 Effect of gold loading..... 74
7.3.1.9 Effect of calcination temperature..... 76
7.3.2 ADSORPTION OF CARBON DIOXIDE ON TiO_2 or Au/TiO_2..... 78
7.3.2.1 Effect of gold on support (TiO_2) when CO_2 is adsorbed at -80°C.....78
7.3.2.2 Effect of gold on support (TiO_2) when CO_2 is adsorbed at room temperature.....80
7.3.2.3 Effect of heating rate..... 81
7.3.2.4 Adsorption of carbon monoxide or carbon dioxide on 1wt% Au/TiO_2..... 84
7.4 POWDER X - RAY DIFFRACTION (PXRD)..... 86
7.4.1 EFFECT OF GOLD ON ANATASE – RUTILE PHASE TRANSFORMATION..... 86
7.5 REFERENCES..... 87
CHAPTER 8..... 88
CONCLUSIONS AND FUTURE WORK..... 88
8.1 FUTURE WORK..... 89
APPENDICES..... 91

SUMMARY

Studies of the adsorption/desorption behaviour of CO and CO_2 on supported gold catalysts are of interest in aiding our understanding of the catalytic oxidation of CO on such solids. The adsorption of carbon monoxide and carbon dioxide on 1.0, 2.0 and 3.0wt% Au/TiO_2 has been investigated by using temperature programmed desorption (TPD). Temperature programmed desorption was used in this work to study the interaction of carbon monoxide or carbon dioxide with the surface of the catalyst. TPD set-up was used in some cases with a methanator in order to improve sensitivity.

Gold highly dispersed on titanium dioxide was prepared by deposition precipitation method. Gold chloride was used as gold precursor and sodium borohydride was used for complete reduction of Au^{3+} to Au^0 during the preparation of these catalysts. The catalysts were characterized by temperature-programmed desorption and powder x-ray diffraction in order to see the effect of gold on the structural properties of titanium dioxide and to attempt to characterize any crystalline gold present.

There are two approaches involved in this work, using adsorption either at low temperature (approximately -80°C) or at room temperature. After calcination of the catalyst to be examined, the reactor was allowed to cool. Adsorption was done at -80°C using a cool bath prepared from liquid nitrogen and acetone mixture. The reactor was immersed in the bath for adsorption to take place at -80°C for 30 min. The computer was programmed to record desorption process from adsorption temperature (-80°C) to room temperature by natural warming.

Alternatively, the calcined sample was cooled to room temperature and adsorption took place at room temperature. After adsorption, the samples were heated from adsorption temperature to 400°C (unless otherwise stated) at 10°C/min. through a temperature programmer in helium/hydrogen (methanation) flow and desorption process was recorded.

The results showed that both CO & CO_2 are weakly bound to the surface of gold/titania composite material as evidenced by a CO desorption temperature maximum of 118°C and a CO_2 desorption temperature maximum of 108°C. Both CO and CO_2 are physically adsorbed on 1wt% Au/TiO_2 composite material. The activation energies of desorption for both CO and CO_2 are identical, 6.0 kJ/mol. The activation energy of desorption showed that both carbon oxides are physically adsorbed on gold supported on titanium dioxide. This study only indicates that CO and CO_2 are physically adsorbed, further experiments which involve chemisorption of CO and CO_2 can be performed.

By increasing gold loading from 1.0 to 2.0 and 3.0 wt% increased the intensity and the number of desorption peaks and consequently influenced the number and type of adsorption sites present in the catalyst.

The effect of the flow rate variation was studied on the desorption curves and the results showed that the amount of the desorbing component is lower at higher flow rates.

Carbon monoxide desorption curve is very similar to carbon dioxide one, this brings us to the conclusion that CO is oxidized to CO_2 on 1wt% Au/TiO_2 composite materials. No mass spectrometry was connected to the TPD system, it is not easy to identify the type of gas desorbing from these solid materials.

The number of gold perimeter sites was calculated from the average gold particle size and the gold loading and found to be $1.0x10^{18}$ /g for 1wt% Au/TiO_2. This figure is close to the minor contribution to adsorption on 1wt% Au/TiO_2 measured as $4.9x10^{18}$.

The deposition of 1.0 wt% gold nanoparticles on titania support inhibited the anatase – rutile phase transformation as confirmed by Powder X-Ray Diffraction results.

CHAPTER 1

INTRODUCTION

In this chapter, the general aspects of gold supported catalysts are discussed, but specific attention will be given to gold supported on titanium dioxide. Also discussed are the properties, uses and morphology of gold. A brief background of general catalysis is reported as well. Also reported is the role of gold in environmental catalysis.

1.1 CATALYSIS

The name 'catalysis' was coined by Berzelius in 1836. He concluded that besides 'affinity' a new force is operative, the 'Catalytic force'. Reaction occurred by catalytic contact. The word 'catalysis' stems from Greek: it has the sense of 'down' and 'loosen'. At that time affinity was known as a chemical driving force, but no understanding existed, on a molecular level, of reaction rates. Catalysis as a tool for carrying out reactions had already been exploited much earlier. It has been applied for thousands of years in processes such as fermentation [1].

Among the first industrial catalytic processes were a few inorganic oxidation processes, viz. the Deacon process (oxidation of hydrochloric acid into chlorine) and the formation of sulphuric acid. These processes were developed before a scientific basic of chemical reactivity was established. Only after the formulation of the theory of chemical equilibria by van't Hoff did a framework for catalyst development became available [1].

Catalysis has made major contributions to many areas of chemical industries. Most of the products in chemical industries are manufactured through catalysis and moreover, many of the difficulties which confront us today, problems of energy, natural resources,

pollution are problems which are amenable to solution by catalysis [2]. It plays an important role in pollution problems, not only in removal of pollutants such as NO_x, CO and sulphur compounds, but also in improving the selectivity of manufacturing processes so that undesirable by-products are not generated. Studying catalysis is therefore an academically valuable exercise for students since it demonstrates clearly the essential unity of scientific and technological problems. Most chemical processes involve the use of catalysts. Therefore catalysis and catalyst development form one of the cornerstones of successful chemical products [3]. Catalysis plays an important role in the manufacture of wide range of products: wine, soap, beer, fertilizers and herbicides from gasoline and plastics, which would otherwise be unobtainable or prohibitively expensive.

The catalytic systems can be divided into two distinct categories, homogeneous and heterogeneous catalysis. When the catalyst is of the same phase as the reactants and no phase boundary exists, we speak of homogeneous catalysis. When a phase boundary separates the catalyst from the reactants we speak of heterogeneous catalysis i.e. the catalyst, the reactants and the product are in different phases. There is however one extremely important group of substances which cannot be accommodated within this classification. Enzymes are neither homogeneous nor heterogeneous catalysts; they are large, complex organic molecules, usually a protein. In heterogeneous catalysis, we are concerned with the specific chemical properties of the surface of a chosen substance. These of course reflect the chemistry of the bulk solid and some useful insight into the catalytic activities of surfaces is gained from knowledge of the bulk properties of the solid. The catalyst is usually a solid and the reactant, a gas or liquid. These catalysts are environmentally friendly with fewer disposal problems.

It has been clear to everyone that in recent years the interest in gold catalysis is booming [4]. Gold catalysts exhibit potential applications of both industrial and environmental importance. Titania as one of the best and most widely used supports for gold deposition since it is possibly to obtain a high dispersion of the gold phase producing very active catalysts. Gold supported on titania has been used in this work, specifically to study the

effect of gold on the adsorption of carbon monoxide and carbon dioxide as revealed by TPD (temperature programmed desorption).

1.2 WHEN GOLD IS USED AS A CATALYST

Bulk gold has been known as chemically inert, but small gold particles appear to be extremely active. An example of known catalytic application of gold is in carbon monoxide oxidation at low temperatures, for producing clean H_2 for fuel cells [4]. In this study, we were interested in understanding more about supported gold catalysis, by finding out more about the binding of adsorbate to catalytic surfaces and identify the kinds of active sites present in Au/TiO_2 catalysts using temperature-programmed desorption.

Until the 1980's gold was considered to be an inactive metal for catalysis, and even some of attributed effects were sometimes ascribed to the presence of impurities in the gold samples used. It is now known to be extremely active for some reaction if deposited on certain supports [5].

Gold is known as one of the most stable metals among the elements which are resistant to oxidation and other aggressive environments. This is why the discovery of gold being a very active catalyst when highly dispersed made a great impact on the scientific community. Gold has been used as second component in platinum- based alloys, the gold being considered as nonmiscible with platinum and segregated to the platinum surface [6, 7]. Turkevich produced gold films of uniform size as early as 1972 [8] and Galvagno and Parravano investigated the activity of gold in oxygen/hydrogen transfer reactions [9, 10] as well as in the NO reduction reaction by hydrogen [11], but gold was known as one of the least reactive metals [12]. The inactivity of gold was attributed to the completely filled 5d shell and the relatively high value of its first ionization potential (9.22eV) [12]. Haruta et al. discovered that gold nanoparticles supported on Co_3O_4, Fe_2O_3 and TiO_2 oxides have exceptionally high activity for CO and H_2 oxidation [13-15], NO reduction [16], water gas shift [17], CO_2 hydrogenation [18] and catalytic combustion of methanol [19] when the dispersion of the gold particles approached 100%. Since the discovery of

the high catalytic activity of gold nanoparticles, several studies have been performed to explain the mechanism of the catalytic action of gold. The still widening research is mainly concerned with the particle size effect and/or metal/support interaction.
Hutchings studied the hydrochlorination of acetylene to vinyl chloride proposed that the standard electrode potential would be a useful measure of catalytic activity [20]. A plot of hydrochlorinated activity versus electrode potential for various metal chlorides resulted in a smooth curve from which it is clear that any metal cation with a higher electrode potential than Hg^{2+} should give enhanced catalytic activity. On this basis gold cations should the most active. Subsequent research by Hutching confirmed this prediction and gold catalysts were found to be about three times more active than the commercial mercuric chloride catalyst. This was the first example of reaction for which gold catalyst exhibited the highest activity [20].

The other demonstrations of gold activity were described by Haruta, at the Osaka National Research Institute in Japan [21]. It was then reported to be extremely active for some reactions if deposited on various supports [5]. Haruta was the first person to show that gold could be effective for CO oxidation at ambient temperature. When gold was coprecipitated with certain metal oxide supports, Haruta found that the resulting catalysts were very active for carbon monoxide oxidation. After testing a range of metal oxide supports, he observed that the best results are obtained with α-Fe_2O_3 and a gold loading of 5%. Indeed, Haruta reported that this catalyst was effective at sub-ambient temperatures and that it was also active at 297K. Haruta's precipitation methods of catalyst preparation result in small metallic gold particles uniformly dispersed on the support. The best results are obtained when these particles are less than ca 5nm in diameter, so that there is sufficient chemical interaction between the metal and the support.

The importance of the metal hydroxide as support seems to be supported by the high activity of Au/Ni $(OH)_2$ in the water gas shift reaction [22].

1.3 CHARACTERISTICS OF GOLD AND ITS USES

Gold:

- Symbol = Au
- Atom number = 79
- [Xe] $4f^{14}$ $5d^{10}$ $6s^{1}$
- Density = 196,97 g/mol
- Metallic radius = 144,20 pm
- Melting point = 1337 K
- Boiling point = 3081 K

Gold, an element long associated with wealth, this metal is currently the focus of active research programs worldwide for a broad range of applications. Gold nanoparticles for catalysis can be prepared on solid support materials by a variety of conventional methods and these methods yield a wide variation in particle size and catalyst efficiencies for benchmark reactions, such as the oxidation of carbon monoxide (CO) to CO_2 [23].

Gold is unique among the metallic elements because of its resistance to oxidation and corrosion: it has been used in coinage and in jewellery for such some time. Platinum was found to be a very versatile catalytic metal and is widely used in commercial applications both for chemical processing and pollution control, notably in automobile exhaust catalytic systems [23]. Gold is unique in a number of ways: it is the most electronegative metal as compared to selenium [24]. Its electron affinity is actually greater than that of oxygen. It readily forms alloys with other metals [25, 26] and intermetallic compounds of definite composition with copper, aluminium, tin and titanium [26]. It exhibits all the properties of the metal in terms of lustre, hardness, ductility, malleability, and high thermal and electrical conductivity.

Gold will not react directly with other electronegative elements such as sulphur or oxygen, and it only dissolves in hydrochloric acid when a strong oxidizing agent such as

nitrate ion is present. There is considerably more gold than platinum group metals (PGMs) in the world, gold is abundant than platinum.

The high conductivity, stability and inertness of gold resulted in it being used in electrical circuitry and recent advances in gold nanotechnology signal exciting new developments. Gold is also used for infrared reflective coatings on glass for aircraft cockpit/space shuttle windows and architectural glass in office buildings. Gold foil is used for decorative gilding coatings in, for example books, church furniture, steeples and statues. This element is also familiar on ceramic tableware and glassware. The use of gold for heterogeneous catalysis could have considerable industrial significance [27, 28]. Industrially traditionally prefers heterogeneous reactions because it is easier to separate catalysts from products once the reaction is complete.

Gold is also used in the micro fuel cell [29]. Essentially, borohydride fuel solutions decompose to produce hydrogen in the presence of platinum or ruthenium. Gold is beneficial because it is relatively unreactive to this decomposition reaction while being suitably active to the desired borohydride oxidation reaction [30].

One of the most exciting things about catalysis by gold is the 'light off' temperatures that are achieved (that is the temperature at which the catalyst becomes functional). Potentially, gold catalysts operate best in the temperature range 200-350K compared to a platinum catalyst's optimum performance in the range 400-800K [31]. Gold catalysts have already been used commercially in Japan for the removal of the odours from toilets. Gold alloys catalysts are also used in the commercial production of vinyl acetate monomer (VAM).

The following reactions have been shown to be affectively catalysed by supported gold catalysts:

- Carbon monoxide oxidation including selective oxidation in a hydrogen stream.
- Catalytic combustion of hydrocarbons.

- Water gas shift.
- Oxidative removal of mercury.
- Selective oxidation e.g. epoxidation of olefins.
- Selective hydrogenation, e.g. of alkynes and dienes to mono olefins.
- Removal of CO from hydrogen streams.
- Hydrogen sulphide and sulphur dioxide removal.
- Ozone decomposition.
- Reduction of NO_x with propene, carbon monoxide or hydrogen.
- Hydrogen + oxygen reaction to give hydrogen peroxide.
- Oxidation of glucose to gluconic acid.
- Vinyl acetate synthesis from ethane, acetic acid and oxygen.

1.4 CRYSTAL STRUCTURE AND MORPHOLOGY

In the bulk form gold has the face centred cubic (fcc) structure (fcc), and the occasional rare crystals of native gold shows the highly symmetrical cubic, octahedral or rhombododecahedral crystal forms accompanying with the fcc structure [32]. This generalization is only true for the particles of about 10 nm in size. For particles smaller than that (between 1 and 10 nm) the situation is even more complicated [33], the structure of gold changes at the nanosize. Many attempts have been done to predict the structure of gold nanoparticles using molecular dynamics or other calculations, but there is not yet complete agreement between the results of the calculations and of the experimental measurements, with conflicting claims being made for icosahedral or decahedral quasicrystal structures, amorphous structures, or octahedra, cuboctahedra and truncated octahedra based on fcc packing. The icosahedral and decahedral clusters have five-fold symmetry, and for nano-scale particles, the icosahedron in particular appears to form an efficient compromise between surface area and packing density [34], whereas certain decahedra have re-entrant facets, and are said to offer a compromise between surface area and strain energy [33]. Icosahedral clusters have a theoretical packing density of 68.8% in contrast to the 74% of the fcc structure. Examples of the three shapes mentioned are

given in Figure 1.1 However, other non-crystalline configurations, which are resistant to change in position or condition besides icosahedra are possible, and they include low symmetry clusters based on 38 to 55 atoms [34] and Marks decahedra, based on 75, 77, 101 and 146 atoms [33]. Several articles like Cleveland et al. [33] have grouped all of the non-crystallographic structures below together as 'decahedral'. Some theoretical studies have concluded that it is these, practically amorphous, clusters that are most stable [34].

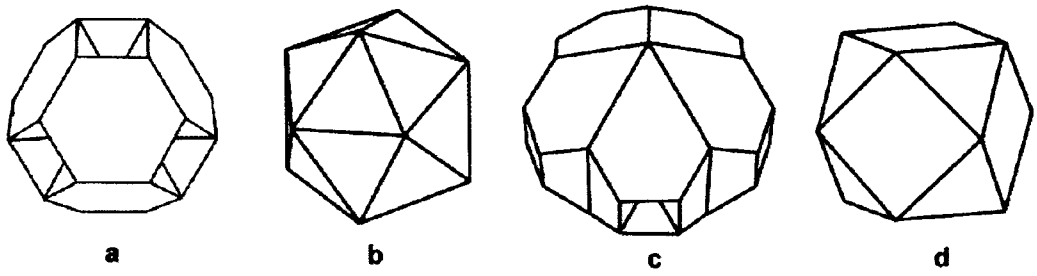


Figure 1.1 Some shapes of gold nano-particles, (a) truncated octahedron, (b) icosahedron, (c) Marks decahedron and (d) cuboctahedron [31].

1.5 ROLE OF GOLD IN ENVIRONMENTAL CATALYSIS

1.5.1 BACKGROUND

Big cities started to experience air quality problems as early as 13^{th} century and up to mid 20^{th} century, not only because of industrial activities but also because of the increasing number of cars [35]. Photochemical air pollution was discovered in the Los Angeles area in the mid 1940s [36]. High concentrations of ozone (O_3) and associated impact on human health has been a major problem in the world. An increase in tropospheric ozone was observed over the past century [37- 43] for example in the Montsouris in France from 1876 to 1910 and in other cities. The huge increase in O_3 was found to be resulting from NO_x emissions produced from industrial activities [36].

Though the mass production of cars gives tremendous personal mobility, several cities were known to be the major source of the man-made emissions [44]. Photochemical reactions of hydrocarbons and nitrogen oxide from car exhaust were known to form photochemical smog and ozone (equation (1)) [36]. The oxidation of fuel to carbon dioxide (equation (2) was not complete. Unburned hydrocarbons, aldehydes, ketones, carboxylic acid and large amounts of carbon monoxide (equation (3)) were also present in the exhaust gases. Large amounts of carbon monoxide were formed. Nitrogen and oxygen in the car exhaust reacted to partially form NO, nitric oxide (equation (4)). The combination of NO and any of its oxidised forms e.g. nitrogen dioxide (NO_2), is referred to as NO_x resulted in several thousand parts per million present in the exhaust gas [36].

The three major primary pollutants in the exhaust gas were found to be hydrocarbons (HC), NO_x and CO respectively. It was understood that the origin of photochemical smog was associated with the primary pollutants from the cars which resulted in formation of large amounts of ozone. The increase in concentration of ozone, which is a strong irritant, has been attributed to an increase in NO_x emissions associated with the switch to fossil fuels during the industrial period [36].

$$HC + NO_x + h\nu \rightarrow O_2 + \text{other products} \quad (1)$$

$$4H_mC_n + (m + 4n)O_2 \rightarrow 2_mH_2O + 4_n CO_2 \quad (2)$$

$$4H_mC_n + (m + 2_n)O_2 \rightarrow 2_mH_2O + 4_nCO \quad (3)$$

$$N_2 + O_2 \rightarrow 2NO \quad (4)$$

In addition, a massive influx in air containing natural ozone from the stratosphere contributes to tropospheric ozone [43, 45].

In mid 1960s, levels of tailpipe pollutants from America cars affected the air quality very seriously and there were typically HC 15g $mile^{-1}$; CO 90g $mile^{-1}$ and NO_x 6 g $mile^{-1}$ respectively [46]. Engines were modified, but this could not alone meet the demands of 1970 Clean Air Act that was designed to make significant improvements in air quality over a reasonable period of time [47].

These problems resulted in development of catalytic systems that could convert HC, NO_x and CO to less harmful products such as carbon dioxide, water and nitrogen.

1.5.2 WAYS OF CONTROLLING THREE POLLUTANTS (NO_x, CO and HC's)

1.5.2.1 Early NO_x control systems

The three pollutants (NO_x, CO and HC) were controlled in a two stage process. Acres and Cooper found the method of controlling NO_x from the car engines by reducing it over a platinum/rhodium catalyst [47]. This was done in the rich reducing exhaust gas before air was added to permit oxidation of the reducing HC and CO species over an oxidation catalyst [47]. The system shown in figure 1.2 was initially used to lower the HC and CO emissions, and it was modified with air injection after a catalyst operation under rich conditions to reduce NO_x and oxidise HC and CO in a second stage.

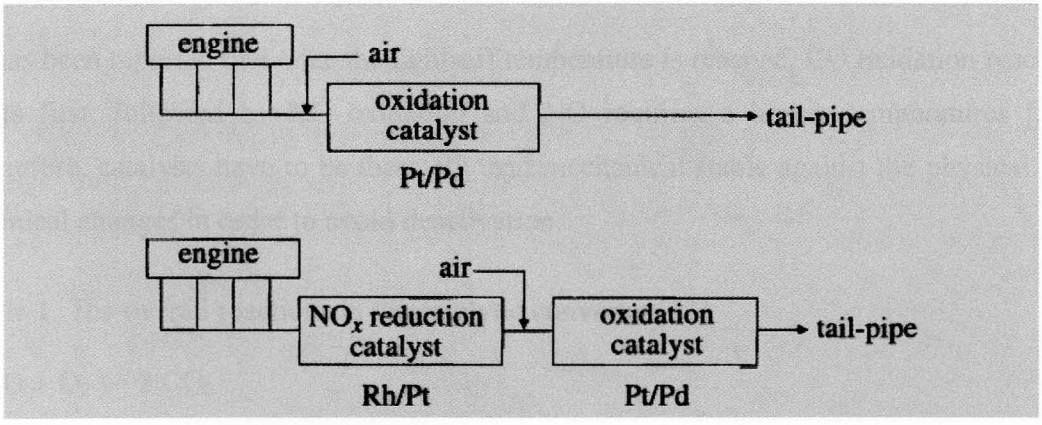


Figure **1.2** Schematic arrangement of oxidation catalysts and air injection point used initially to lower HC and CO emissions, and the later modification using air injection with a catalyst operating under rich conditions to reduce NO_x and oxidise HC in a second stage [48].

Rhodium has proven to be an efficient catalyst for NO_x reduction [49] whereas palladium and platinum metals are effective in CO and hydrocarbon oxidation reactions.

Three-Way Catalysts were developed because they are capable of removing the major pollutants HC, CO and NO_x simultaneously [36].

1.5.2.2 DEVELOPMENT OF THREE - WAY CATALYSTS

The US Clean Air Act of 1970 led to the introduction of auto-exhaust catalysts, the main objective being to reduce the emission of CO and unburnt hydrocarbons (HC) [50]. The so-called Three-Way Catalyst (TWC) have been used since 1979. With the TWC, several oxidation and reduction reactions take place in the catalytic converter, which is capable of removing the major pollutants HC, CO and NO_x simultaneously. Three-Way Catalysis is possible if and only if fuel/air ratio in the gas mixture is stoichiometric with the catalyst containing rhodium and platinum as key components [50]. This development provided a more effective way of controlling HC, CO and NO_x than the earlier two catalyst system [48].

It has been reported that once the light-off temperature is reached, CO oxidation reaction starts first, followed by HC oxidation and NO requires a higher temperatures [51]. Therefore, catalysts have to be thermally and mechanical stable against the physical and chemical changes in order to avoid deactivation.

Table 1. The overall reactions in the catalytic converter [52].

$2\ CO + O_2 \rightarrow 2\ CO_2$

$4\ C_xH_y + (4x + y)O_2 \rightarrow 4x\ CO_2 + 2y\ H_2O$

$2\ NO + 2\ CO \rightarrow N_2 + CO_2$

Three-Way Catalysts are made up of a honey-comb like monolithic structure with the monolith support made of either stainless steel or ceramic material [53]. The monolith contains small channels which are washcoated with the active catalyst material

impregnated on those channel walls. The main compounds in the washcoat are base-metal oxides, such as alumina, ceria and zirconia. Ceria was added to promote the low temperature water gas shift reaction, to store oxygen under fuel deficient conditions, to stabilize precious metal dispersion against thermal damage and to alter carbon monoxide oxidation kinetics [52].

Bulk gold was typically known as chemically inert, but small gold particles appear to be extremely active. Haruta et al.[4] discovered that gold is a very active catalyst for CO oxidation and offered some promise for the substitution of the Three-Way Catalyst in alleviating the car exhaust emissions. Gold has been reported to be active for a number of reactions and an example of known catalytic application of gold is in carbon monoxide oxidation at low temperatures, for producing clean H_2 for fuel cells [4].

1.6 REFERENCES

[1] R. A. van Santen, P.W.N.M. van Leeuwen, J.A.Moulijn, B.A. Averill, Catalysis: An Integrated approach, 2nd Ed. Kluwer Academic Publishers: The Netherlands, 1987.

[2] C.G. Bond, Heterogeneous Catalysis, Principles and Applications, Oxford University Press: New York, 1974, 1987.

[3] J.B. Higgins, Catal. Today **19** (1994) 7.

[4] http://edu.chem.tue.nl/6KM11/files/Project%20reports%202003%202004/Catalysis% 20by%20Gold.pdf 12/05/2005.

[5] M. Haruta, CATTECH **6** (2002) 102.

[6] D.I. Hagen, G.A. Somarjai, J. Catal. **41** (1976) 466.

[7] J.W.A. Sachtler, M.A. van Hove, J.P. Biberian, G.A. Somarjai, Phys. Rev.Lett. **45** (1980) 1601.

[8] J. Turkevich, G. Kim, Science **169** (1970) 873.

[9] D.Y. Cha, G. Parravano, J. Catal. **18** (1970) 200.

[10] J. Schwank, S. Galvagno, G. Parravano, J. Catal. **63** (1980) 415.

[11] S. Galvagno G. Parravano, J. Catal. **55** (1978) 178.

[12] J. C. Bailar, Comprehensive Inorganic Chemistry, Pergamon Press: New York, 1973.

[13] Z. Pászti, L. Tòth, Z.E. Horváth, A. Karacs, G. Petõ, J. Phys. Chem. B **104** (2000) 3183.

[14] M. Haruta, N. Yamada, T. Kobayashi, S. Iijima, J. Catal. **115** (1989) 301.

[15] M. Haruta, Catal. Today **36** (1997) 153.

[16] A. Ueda, T. Oshima, M. Haruta, Appl. Catal. **12** (1997) 81.

[17] D. Andreeva, T. Tabakova, V. Idakiev, P. Christov, R. Giovanoli, Appl. Catal. **169** (1998) 9.

[18] H. Sakurai, M. Haruta, Catal. Today **29** (1996) 361.

[19] M. Haruta, A. Ueda, S. Tsubota, R.M. Torres Sanches, Catal. Today **29** (1996) 443.

[20] G.J. Hutchings, Gold Bull **5** (1971) 11.

[21] http://www.chemsoc.org/chembytes/ezine/2001/thompson_nov01.htm15/15/2005.

[22] A. Andreev, L. Petrov, C. Bonev, G. Kadinov, I. Mitov, Proceedings of the 8th International Symposium on heterogeneous Catalysis, Eds., Varna, (1996)141.

[23] C.G. Bond, Catal. Rev. Sci. Eng. **41** (1999) 321.

[24] N.N. Greenwood, A. Earnshaw, Chemistry of the elements, Pergamon, Oxford, 1984.

[25] W.S. Rapson, Gold Bull. **29** (1996) 141.

[26] M.G. Mason, Phy.Rev. B **27** (1983) 748.

[27] D.T. Thomson, Gold Bull. **31** (1999) 111.

[28] G.C. Bond, D.T. Thomson, Gold Bull. **33** (2000) 41.

[29] http://www.gold.org/discover/sci_indu/presentations/files/munich_2004_poster.pdf 12/05/2005.

[30] World Gold Council, 'CatGold News' issue No. 6 Spring 2004.

[31] http://www.gold.org/discover/sci_indu/gold_catalysts/ 25/05/2005.

[32] H.H. Read, Rutley Elements of Mineralogy, Thomas Murby, Co, London, 26th Edition, 1970.

[33] C.L.Cleveland, U. Landman, T.G. Schaaf, M.N. Shafigullin, Phys. Rev. Letters **79** (199) 1873.

[34] A.L. Mackay, Acta Cryst. **15** (1962) 916.

[35] A.J Haagen-Smit, M.M Fox, SAE Trans. **63** (1995) 575.

[36] www.sciencemag.org.science.vol.276.16/051997.

[37] J. Fishman, P.J. Crutzen, Nature **274** (1978) 855.

[38] J. Logan, J. Geophys. Res. **90** (1985) 10463.

[39] R.D. Bojkov, J Am. Meteorol. Soc. **25** (1986) 343.

[40] A. Volz, D. Kley, Nature **332** (1988) 240.

[41] D. Anfossi, S. Sandroni, S. Viarengo, J. Geophys. **96** (1991) 17349.

[42] A.P. Altshuller, J. Air Pollut. Control Assoc. **37** (1987) 1409.

[43] P.J. Crutzen, Faraday discuss **100** (1995).

[44] A.J Haagen-Smit, M.M Fox, J. Air Pollut. Control Assoc. **4** (1954) 105.

[45] J.R. Holton et al. Rev. Geophys **33** (1995) 403.

[46] Auto Emission Control Systems, Hydrocarbon processing (1971) 85.

[47] G.J.K. Acres, B.J. Cooper, Platinum Met. Rev. **16** (1973) 74.

[48] M.V. Twigg, Phil.Trans R. Soc. A. **363** (2005) 1013.

[49] K.C. Taylor, J.C. Schlatter, J. Catal. **63** (1980) 53.

[50] J.M Thomas, W.J Thomas, Principles and Practice of Heterogeneous Catalysis, VCH Publishers Incl: New York (1996) 577.

[51] R.M. Heck, R.J. Farrauto, Appl. Catal. A: General **221** (2001) 443.

[52] E.S.J. Lox, B.H. Engler, Environmental Catalysis-Mobile Sources, VCH:Weinheim, Germany (1997) 1559.

[53] http://herkules.oulu.fi/isbn9514269543/html/x382.html 19/10/2006.

CHAPTER 2

TITANIUM DIOXIDE (TiO_2)

In this Chapter, the structures of different crystalline forms, namely rutile, anatase and brookite are described. All possess the same empirical chemistry as TiO_2 but each has a different crystal structure. Also discussed are the uses of titanium dioxide with its properties as well as the effect of titanium dioxide as a catalyst support.

2.1 STRUCTURE, PROPERTIES AND USES

Titanium dioxide as a raw material supports industries worth $3 billion annually in the USA alone [1]. Pure titanium dioxide does not occur in nature but is derived from leuxocene ores. It is readily mined in one of the purest forms, rutile beach sand. These ores are the principal raw materials used in the manufacture of titanium dioxide pigment. The first step is to purify the ore, and is basically a refinement step. After purification, the powder is treated (coated) to enhance their performance as pigments.

Titania acts as a photosensitiser for photovoltaic cells, and when used as an electrode coating in photoelectrolysis cells can enhance the efficiency of electrolytic splitting of water into hydrogen and oxygen and can also be used as oxygen sensor.

TiO_2 is primarily used in pigment industry for paints, varnishes, papers, cosmetics and plastics. It is also utilized in catalysts, ceramics, coated fabrics and roofing granules. It is a very useful material which provides diversity of applications especially in photocatalysis and as a catalyst support [2]. Recently, the use of titania has been extended to medical applications such as use in artificial heart valve and in dental

implants [3, 4]. A growing interest in the development of well-structured, porous, high surface area and complex forms of titania based materials has also led to the use of TiO_2 in several novel applications [5].

Titanium dioxide is a ceramic material commonly known as titania. It is applied in enamelling and catalysis [6]. Titania exists in a number of crystalline forms, namely rutile, anatase and brookite. All possess the same empirical chemistry as TiO_2 but each has a different crystal structure. Brookite is rarely used commercially and has an orthorhombic crystal structure (figure 2.3) which spontaneously transforms to rutile around 750°C [6]. The most important ones are anatase and rutile. Anatase is metastable with respect to rutile and has a tetragonal crystal structure in which the Ti-O octahedra share four corners as shown in figure 2.1. Anatase coarsens and transforms to rutile [7]. The stability of anatase with respect to rutile is particle size dependent [7], with a stability reversal occurring at ~ 10 – 15nm diameter.

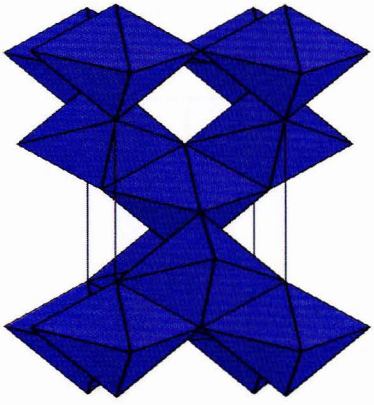


Figure 2.1 A diagram of the anatase crystal [8]

Rutile is considered the most stable form of TiO_2 at ambient conditions [9]. It has a crystal structure similar to that of anatase with the exception that the octahedra share four edges instead of four corners. This leads to the formation of chains, which are subsequently arranges in a four-fold symmetry, as shown in figure 2.2.

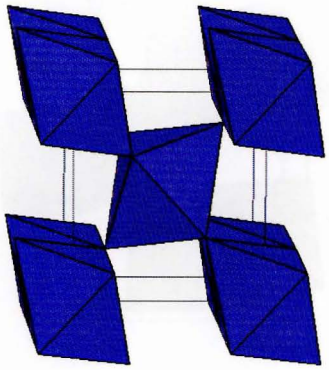


Figure 2.2 A diagram of the rutile crystal [8]

From the two figures above, we can see that rutile structure is more densely packed than that of anatase.

Table 2.1 Comparison of anatase & rutile [10]

Phase	**Refractive index**	**Density (g cm^{-3})**	**Crystal Structure**
Anatase	2.49	3.84	Tetragonal
Rutile	2.903	4.26	Tetragonal

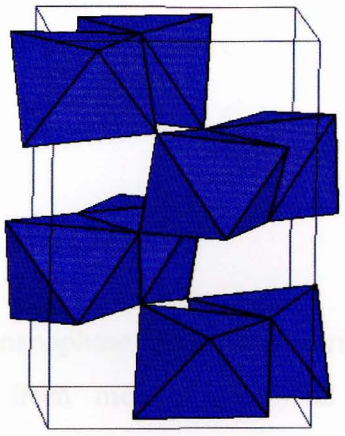


Figure 2.3 A diagram of the brookite crystal [8].

2.2 DEGUSSA P25

Degussa P25 is the kind of titanium dioxide used in this study. It is produced from titanium tetrachloride by flame hydrolysis and has no pigment characteristics because its particles are very fine. It can be purified by distillation and is originally hydrophobic. It is normally used if a high surface area is wanted in order to attain a certain technical effect and is known to consist of 80% anatase and 20% rutile. However, there are suggestions that titanium dioxide P25 consists of separate rutile and anatase crystals [11]. Its surface area is approximately 50 m^2/g and its density was found to be 130 g/L according to DIN ISO 787/X1 [12]. Many researchers claimed that it is a good photocatalyst. Although it is thought that anatase, the major component, is mainly responsible for the overall photocatalytic activity, clear evidence of this has not been obtained. Porter investigated that the rutile to anatase ratio, the anatase and rutile crystalline sizes increase with increasing calcination temperature but the surface area decreases [13].

In this study, it has been discovered that, the anatase, which is the major component, coarsens and transforms to the rutile phase at higher calcination temperature (400°C). As

the calcination temperature increases to 500°C and 600°C, the rutile-anatase ratio increases. AT 700°C (calcinations temperature), we noted that all the anatase phase transforms to the rutile phase.

2.3 PHASE TRANSFORMATION

At high temperatures many nanophase ceramic materials undergo solid-solid phase transitions as they convert from metastable crystal structure to a more stable thermodynamic phase. In the case of TiO_2, the anatase to rutile transition is observed to occur between 500-900°C. When the anatase phase of TiO_2 is heated at high temperature, it normally becomes coarse and subsequently transforms into the rutile phase [14]. Zang and Banfield showed that the phase transformation is reconstructive and requires the repoisoning of Ti cations and a change in the oxygen arrangement [9].

Farrell has reported that the general accepted theory of phase transformation is that two Ti-O bonds break in the anatase structure allowing rearrangement of Ti-O octahedra, which leads to a smaller volume and a rutile structure [15]. He also added that the breaking of these bonds is accelerated by lattice disruption which is introduced in a number of ways including the addition of dopants, variation in the atmosphere and method of preparation [15]. In addition to this he claimed that the free energy of the rutile is lower than that of anatase at all temperatures.

Zhang and Banfield [16] studied the phase transformation behaviour of nanocrystalline aggregates during their growth for isothermal and isochronal reactions by using XRD. They suggested that transformation sequence and thermodynamic phase stability depend on the initial particle sizes of anatase and brookite. They concluded that, for equally sized particles, for particle size <11 nm, anatase was thermodynamically stable, for particle size between 11 nm and 35 nm, brookite was stable, and for particle size >35 nm, rutile was stable. They cautioned that, for real samples, the particle sizes of different phases were not equal, which could alter the direction of initial transformation. They

concluded that the energetics of these polymorphs were sufficiently close that they could be reversed by small differences in surface energy [16, 17].

Zhang et al. [18] measured micro-Raman spectra of nano-sized TiO_2 powders prepared by vapour hydrolysis. They obtained amorphous TiO_2 at 533 K and predominantly anatase at 873–1 173 K. The anatase–rutile transformation temperature depended on particle size and was complete at ≈1,323 K [18]. They noted that the phase transformation of amorphous TiO_2 was a two-step process: amorphous to anatase followed by anatase to rutile. They proposed that the rutile formation started at the surface and migrated into the bulk. They also noted that the brookite impurities, detected by Raman spectroscopy but not by XRD, were present on the anatase surface.

Talavera and co-workers [19] showed that the anatase-rutile phase depends strongly on the kind of cation used to dope the titania material prepared by sol-gel method. They studied the effect of dopants on the thermal and structural properties of the materials. When different metals were used, the anatase to rutile phase transition occurred at different temperatures. They concluded that, the temperature range where the anatase phase exists can be controlled by choosing the appropriate dopant.

The anatase–rutile transformation depends on impurities, grain size, reaction atmosphere, and synthesis conditions [20-25]. Zhang and Banfield [20] reported that the anatase - rutile phase transformation occurred at higher temperature with the addition of Al_2O_3. They attributed this to suppression of coarsening caused by surface diffusion. Yoshinaka et al. [22] found that the anatase–rutile phase transformation occurred at higher temperature with the addition of SiO_2. Yang et al. [23] showed that synthesis conditions (chemicals/peptizing agents) affect the crystallinity and anatase - rutile phase transition temperature. Zaban et al. [24] noted that the surface structure of TiO_2 is affected by the preparation conditions.

Ahonen et al. [25] studied the effect of gas atmospheres (nitrogen and air) and temperature on the crystal structure and specific surface area. They observed that anatase synthesized in air transformed to rutile at 973 K, whereas anatase synthesized in nitrogen

persisted to 1,173 K. Gouma and Mills [26] studied the anatase - rutile phase transformation in commercial TiO_2 powders with an average particle size of 100 nm. Using transmission and scanning electron microscopy, they concentrated on the structural evolution (shape and morphology) of the particles. They proposed that rutile plates were formed initially by a shear force and subsequent coarsening involved interactions between the transforming particle and surrounding anatase particles [17].

A new modification of nanosized titanium oxide by delaminating precursor crystals of layered titanates into their elementary layers has been reported [27, 28] (figure 2. 4). The titania nanosheets exhibit very sharp and intense absorption of ultraviolet (UV) light, which is markedly blue shifted from that of bulk titania [29]. These nanosheets show photochemical reactivity under UV irradiation, i.e. photocatalytic decomposition of organic substances and photoinduced hydrophilicity [30].

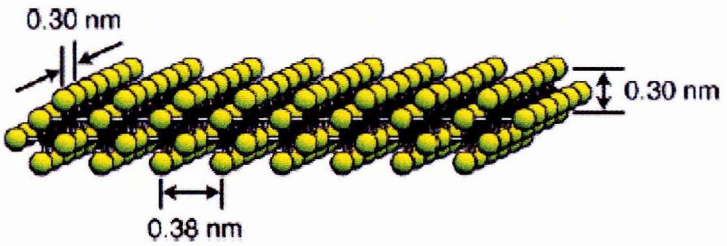


Figure 2.4 Atomic architecture of the nanosheet crystallites of TiO_2

2.4 WHEN TITANIA IS USED AS THE CATALYST SUPPORT

TiO_2 is one of the best and most used supports for gold deposition since it is possibly to obtain a high dispersion of the gold phase producing very active catalysts [31]. The acid-base properties of TiO_2 powders have been widely studied and they show a different behaviour (acid, amphoteric or basic) according to the crystalline phase (anatase or rutile) and the method of preparation [32,33,34].

Earlier work has already demonstrated that the nature of the support has a decisive role in the activity of gold catalysts. Alumina & manganese supported gold were found to be significantly more active than silica-supported gold [35]. It is found that there is evidence that the interaction between the support and the gold particles has an important influence on catalytic performance [36]. Although both gold itself and pure titania are inactive for carbon monoxide oxidation below 500K, both 1% Au/TiO_2 and gold powder with titania deposited on its surface are active at 298K [32]. A rate of 2.3 x 10^{-6} $mol.g^{1}cat\ s^{-1}$at 313K was recorded for 1% Au/TiO_2 catalyst [32], which is significant improvement on 6.8 x 10^{-8} $molg^{-1}cat\ s^{-1}$recorded earlier for 1.8 % Au/SiO_2 at the same temperature [37]. Gold is catalytic provided that gold particles are small (<5 nm) and supported on metal oxides. Gold supported on TiO_2 exhibits remarkable catalytic properties in the reaction of CO oxidation at sub-ambient temperature when gold particle size is 2-3 nm [38]. The challenge is to achieve production of such small particles. This was effected by Haruta et al. [39] by the method of deposition-precipitation with NaOH (DP NaOH). In this method the gold precursor, typically chloroauric acid ($HAuCl_4$), is brought out of solution in the presence of a suspension of the support by raising the pH in order to precipitate Au $(OH)_3$. The surface of the support acts as a nucleating agent so that if the method is properly performed, and local high concentrations of alkali are avoided, the active precursor is selectively deposited on the support surface. The surface properties of the support must therefore play a predominant role in the gold deposition. The nature of the support is a key factor that strongly affects the final dispersion of gold [40, 41]. Small metal particles are unstable with respect to massive gold, so the support must present a suitable surface area which keeps them apart. Moreover, a strong interaction between the gold particles and the surface of the support is required to stabilize them and to avoid sinterisation, essentially in the calcination step.

The properties of highly dispersed gold nanoclusters supported on metal oxides catalysts depend on the support [42], synthesis method [43, 44], and pretreatment conditions [45, 46].

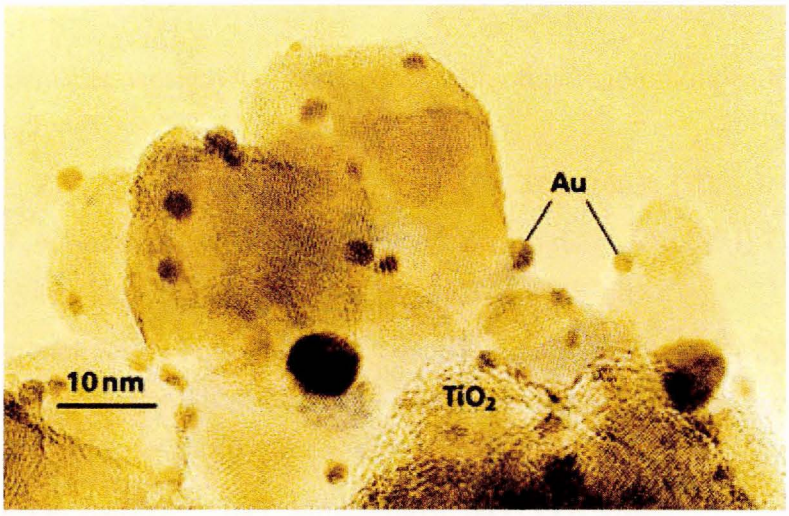


Figure 2.5 Transmission electron micrograph (TEM) of Haruta's Au/TiO_2 supported gold catalysts prepared by Deposition precipitation [47].

Haruta reported that method of preparation affects the shape of gold particles for example coprecipitation and deposition - precipitation produced hemispherical gold particles that are strongly attached to the oxide support (TiO_2) by their flat planes, and claimed this was the reason for their high activity [48]. A typical TEM is shown above in Figure 2.5.

2.5 REFERENCES

[1] http:/minerals.er.usgs.gov/minerals/pubs/commodity/titanium/index.html#mcs U.S 13/06/2005.

[2] T.Z. Ren, Z.Y. Yuan, B.L. Su, Chem.Phys. Lett. **374** (2003) 170.

[3] P.J. Li, T. Kokubo, K. de Groot, J. Biomed, Material Sci. **28** (1994) 7.

[4] Y. Han, S.H. Hong, K. Xu, Mater. Lett. **56** (2002) 744.

[5] D.M. Antonelli, Y.J. Ying, Angew. Chem. Int. Ed. Engl. **34** (1995) 2014.

[6] I.J. McColm, Ceramics Science for materials Technologists "Leonard Hills" Chapman and Hall, New York, 1983.

[7] H. Zang, J.F. Banfield, Amer. Mineralogist, **84** (1999) 528.

[8] http://ruby.colorado.edu/~smyth/min/tio2.html18/05/2005.

[9] H. Zhang, J.F. Banfield, J. Mater. Chem. **8** (1998) 2073.

[10] http://www.azom.com/details.asp?ArticleID=1179 07/06/2005.

[11] A .K. Datye, G. Riegel, R. J. Bolton, M. Huang, R.J. Prairie, Solid State Chem. **115** (1995) 236.

[12] Degussa Aerosil, Silane, Technical Bulletin Fine particles, Number 80.

[13] C.K. Chan, J.K. Porter, Y.G. Li, W. Guo, J. Amer. Cer. Soc. **82** (1999) 566.

[14] H. Zhang, J.F. Banfield, Amer. Mineralogist Chem. **84** (1999) 528.

[15] K. A. Farrell, "Synthesis Effects on Grain Size and Phase content in the Anatase-Rutile TiO_2 system", Thesis for the Degree of Masters, submitted to the Faculty of the Worcester Polytechnic Institute, February 2001.

[16] H.Z. Zhang, J.F. Banfield, J. Phys. Chem. B **104** (2000) 3481.

[17] http://www.pubmedcentral.nih.gov/articlerender.fcgi?artid=128553 07/06/2005.

[18] Y. Zhang, C.K. Chan, J.F. Porter, W. Guo, J. Mater. Res. **13** (1998) 2602.

[19] R. Rodriguez-Talavera, S. Vargas, R. Arroyo - Murillo, R. Montiel-Campos, E. Haro-Poniatowski, J. Mater. Research. **12**(1997) 439.

[20] H. Z. Zhang, J. F. Banfield, J. Mater. Res. **15** (2000) 437.

[21] K. Okada, N. Yamamoto, Y. Kameshima, A. Yasumori, J. Am. Ceram. Soc. **84** (2001) 1591.

[22] M. Yoshinaka, K. Hirota, O. Yamaguchi, J. Am. Ceram. Soc. **80** (1997) 2749.

[23] J. Yang, S.Mei, J.M.F. Ferreira, J. Am. Ceram. Soc. **83** (2000) 1361.

[24] A. Zaban, S.T. Aruna, S. Tirosh, B.A.Gregg, Y. Mastai, J. Phys. Chem. B **104** (2000) 4130.

[25] P. Ahonen, E.I. Kauppinen, J.C Joubert, J.L. Deschanvres, G. Van Tendeloo, J. Mater. Res.**14** (1999) 3938.

[26] P.I.Gouma, M.J. Mills, J. Am. Ceram. Soc. **84** (2001) 619.

[27] R. Conanec, R. Marchand, Y. Laurent. High Temp.Chem. Process **1** (1992)157.

[28] E. Guéguen, S. Delsarte, V. Peltier, R. Conanec, R. Marchand, Y. Laurent, P. Grange, J. Eur. Ceram. Soc. **17** (1997) 2007.

[29] M.A. Centeno, M. Debois, P. Grange, J. Phys. Chem. B **102** (1998) 6835.

[30] L. Legendre, R. Marchand, Y. Laurent. J. Eur. Ceram. Soc. **17** (1997) 1813.

[31] M. Daté, Y. Ichihashi, T. Yamashita, A. Chiorino, F. Bocuzzi, M. Haruta, Catal. Today **72** (2002) 89.

[32] M. Primet, P. Pichat, M.V. Matheiu, J. Phys. Chem. **75** (1971) 1221.

[33] G. Busca, H. Saussey, O. Saur, J.C. Lavalley, V. Lorenzelli, Appl. Catal. **14** (1985) 245.

[34] G.D. Parfitt, Prog. Surf. Membr. Sci. II **11** (1976) 181.

[35] S. Galvagno, G. Parravano, Phys. Chem. **83** (1979) 894.

[36] D.I. Hagen, G.A. Somarjai, J. Catal. **41** (1976) 466.

[37] S.D. Lin, M. Bollinger, M.A. Vannice, Catal. Lett. **17** (1993) 245.

[38] M.A. Bollinger, M.A. Vannice, Appl. Catal. B, Environ. **8** (1996) 417.

[39] S. Tsubota, M. Haruta, T. Kobayashi, A. Ueda, Y. Nakahara, Stud. Surf. Sci.Catal. **72** (1991) 695.

[40] M.A. Centeno, M. Paulis, M. Montes, J.A. Odriozola. Appl. Catal. A **234** (2002) 65.

[41] A.I. Kozlov, A.P. Kozlova, H. Liu, Y. Iwasawa. Appl. Catal. A **182** (1999) 9.

[42] M.M Schubert, S. Hackenburg, A.C. van Veen, M. Muhler, V. Plzak, R.J. Behm, J. Catal. **197** (2001) 113.

[43] M. Haruta, Catal. Today **36** (1997) 153.

[44] A.P. Kozlova, A.I. Kozlov, S. Sugiyama, Y. Matsui, K. Asakura, Y. Iwasawa, J.Catal. **181** (1999) 37.

[45] M. Maciejewski, P. Fabrizioli, J.D. Grunwaldt, O.S. Becker, A. Baiker, Phys. Chem. **3** (2001) 3846.

[46] B. Schumacher, V. Plzak, M. Kinne, R.J. Behm, Catal. Lett. **89** (2003) 109.

[47] http://www.chemsoc.org/chembytes/ezine/2001/thompson_nov01.htm 25/06/2005.

[48] M. Haruta, Catal Today **36** (1997) 153.

CHAPTER 3

PREPARATION OF SUPPORTED GOLD CATALYSTS

After gold supported catalysts have been prepared, they are examined by several techniques for the analysis of their characteristics. Nowadays, there are many techniques available for characterization (an important tool in catalysis) of such catalysts. The techniques commonly used are discussed in this chapter including the methods of preparation and the factors that affect the catalytic activity. The techniques used to study the interaction of the reactant gas and the surface of the catalyst offer tools to investigate the nature of the active site. With such information, we hope to understand catalysis better, so that we can design new and improved catalysts.

3.1 METHODS OF PREPARING SUPPORTED GOLD CATALYSTS

The major parameters for catalyst preparation are the pH, concentration, temperature of an aqueous solution of $HAuCl_4$ and calcination temperature. Figure 3.1 shows the effect of pH on the mean diameter of gold particles. In the study by Okumura it was indicated that the acidic solutions below pH 6 could results in the formation of Au particles larger than 10 nm and basic solutions led to diameters smaller than 5nm [1]. The size of gold particle gradually increases with increasing temperature for calcination in air.

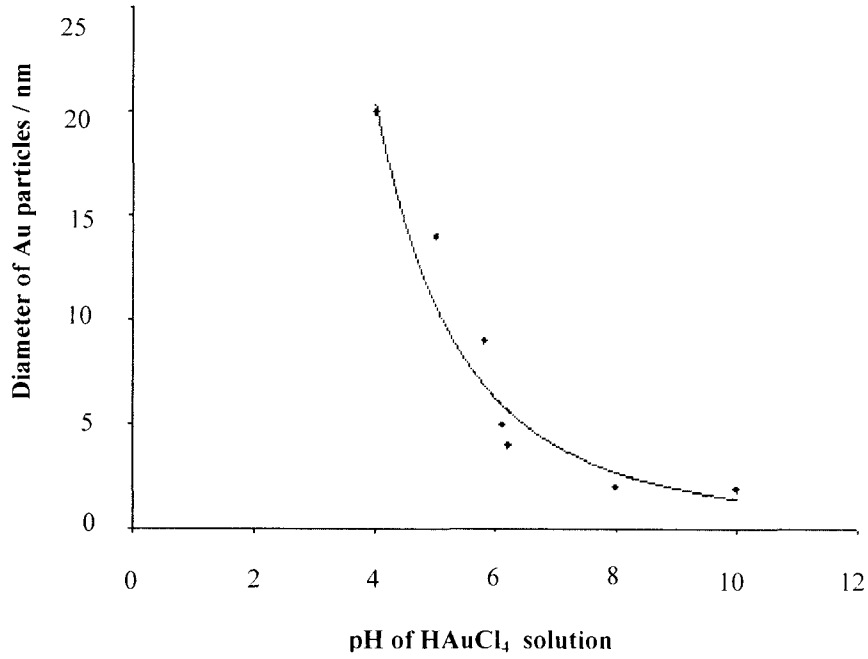


Figure 3.1 The mean diameters of Au particles deposited on TiO_2 as a function of pH of aqueous $HAuCl_4$ [1]

The first reported practical catalysts were created by Haruta [2] in 1987, by the coprecipitation method, using iron, cobalt and nickel oxides precipitated with Na_2CO_3. There are so many ways of getting gold particles in the nanometer size range. The main problem is the creation of small metallic particles that are stable under reaction conditions. Therefore particles are often deposited on a support, which is usually a metal oxide. Even though methods such as chemical vapour deposition (CVD), sol-gel synthesis or colloidal routes are well established in chemical laboratories, the most often used methods in large scale industry as well as in academic laboratories are the following:

3.1.1 DEPOSITION-PRECIPITATION METHOD [3, 4]

The method of catalyst preparation used in this study is deposition-precipitation method. Among the available methods for preparing supported gold catalysts with high dispersion

of the gold phase, deposition-precipitation is one of the most successful [5-8]. In this method the gold precursor, typically chloroauric acid ($HAuCl_4$), is brought out of solution in the presence of a suspension of the support by raising the pH in order to precipitate Au $(OH)_3$. The surface of the support acts as a nucleating agent so that if the method is properly performed, and local high concentrations of alkali are avoided, the active precursor is selectively deposited on the support surface. The surface properties of the support must therefore play an important role in the gold deposition. The nature of the support is a key factor that strongly affects the final dispersion of gold [9, 10]. Small metal particles are unstable with respect to massive gold, so the support must have a suitable surface area which keeps them apart. Moreover, a strong interaction between the gold particles and the surface of the support is required to stabilise them and to avoid sintering, especially in the calcination step.

The optimal experimental conditions for obtaining gold nanoparticles by the deposition-precipitation method are dependent on the different supports used [11]. This observation reinforces the idea of the critical relationship between the surface support properties and the final gold dispersion achieved. In order to precipitate gold as $Au(OH)_3$ on the surface and not in the bulk of the support, an increase of the local basicity of the surface is required [5].

Deposition-precipitation has the advantage over coprecipitation because all of the active component remains on the surface of the support and is not buried within it. The procedure has been used to prepare a number of supported gold catalysts [12] and is preferred to coprecipitation on the grounds that it gives a narrower particle size distribution. Haruta et al. recommended that the support should have an area of at least 50 $m^2 g^{-1}$ [13].

Taylor and Francis also discovered that deposition-precipitation and coprecipitation are better methods than impregnation. A catalyst consisting of small gold particles (<5 nm) supported on a metal oxide is required for certain reactions such as oxidation of carbon

monoxide at low temperatures. Deposition-precipitation and coprecipitation also provide the desired intimacy of contact between the metal and the support [14].

Deposition-precipitation was found to have a potential advantage over coprecipitation in that the entire active component remains on the surface of the support and none is buried within it. Another advantage is that it gives a narrower particle size distribution of the metal (Au) on the support [5]. Gupta and co-workers also discovered that deposition-precipitation method is easily scalable and can work with any type of support [15]. They reported that, deposition-precipitation by thermal decomposition of urea is a superior synthetic approach compared to conventional methods because it allows complete precipitation of the gold precursor from solution and less than 0.1% gold is left in the liquid phase. Galvagno and the co-workers reported that in the case of coprecipitation more than 50% of gold remains in the solution [16]. According to the results obtained by Gupta and co-workers, 85-90% of gold precursor was left in the liquid phase after coprecipitation procedure was complete. They also added that they believe that deposition-precipitation achieves a complete precipitation of gold precursor because of finer control of the solution pH.

3.1.2 IMPREGNATION [20]

For impregnation, the gold precursor, usually $HAuCl_4$ [17] or $AuCl_3$ [18], is dissolved in water in quantities which correspond to the desired metal loading, followed by wet impregnation of the support material (e.g. SiO_2, TiO_2, ZrO_2) present in powder form or as extrudates. After drying, calcination [19, 20] and a subsequent reduction in hydrogen at elevated temperatures (473–773 K) [21] the final supported gold catalyst is obtained. Application of the more special incipient wetness method is also possible, where the amount of water containing the gold precursor corresponds to the pore volume of the support material.

3.1.3 PRECIPITATION [5, 22]

An aqueous solution of the gold precursor is adjusted to a fixed value of pH ranging from 6-10, the preformed support material is added (deposition-precipitation, DP). Alternatively the support can be precipitated simultaneously (co-precipitation, CP). After further stirring and aging of the solution, the precipitate is dried, washed several times in an appropriate solvent and then filtered, calcined and reduced in a similar manner as for impregnations [23, 24].

3.1.4 ION EXCHANGE AND PREPARATION OF GOLD/ZEOLITE CATALYSTS [3, 4]

The ion exchange method involves cation exchange by which protons or other cations on the surface or within the structure of the support are replaced by cations of the active metal, with the noble elements of group 8-10, to atomically dispersed species, and then after calcination and carefully reduced with hydrogen to very small metal particles [5]. The procedure is especially effective with zeolites [25]. This method has not been used more widely for preparation of small gold particles, the reason being the limited number of cationic gold complexes available e.g. $[Au(en)_2]^{3+}$ & $[Au(NH_3)_2]^{+}$. A number of attempts to put gold species into zeolites has been reported and gold (4%) has been introduced into HY zeolites by cation exchange using $[Au(en)_2]^{3+}$ ion. This was followed by thermal decomposition at 423 K [26]. The material was analyzed by ^{129}Xe nuclear magnetic resonance (NMR), by which it was discovered that 80% of the particles were between 1 and 4 nm in size and few particles larger than 5nm were also seen on the outside of the zeolite crystallites.

3.1.5 VAPOUR-PHASE DEPOSITION AND GRAFTING [3, 13]

In the vapour-phase method, a stream of a volatile compound of gold is transported to a high area support by an inert gas, and it reacts with surface of the support to form a precursor to the active species. Gold acetylacetonate has been used to prepare Au/SiO_2

catalysts in this way [27]. A gold complex in solution reacts with the surface of a support to form species capable of being converted to a catalytically active form [13], this occurs in the grafting method.

3.1.6 CO-SPUTTERING [13]

In an oxygen containing atmosphere, gold and metal oxide are simultaneously sputter-deposited onto a substrate, leading to the formation of a thin film. The film is then annealed in air.

Coprecipitation (CP), Deposition-precipitation (DP), co-sputtering, liquid-phase grafting can produce highly dispersed gold particles, which exhibit unique catalytic nature in many different reactions depending on the type of metal supports. Au supported on insulating metal oxide such as Al_2O_3 & SiO_2 was less active than Au/TiO_2, Au/Fe_2O_3 and Au/NiO [28] for low temperature CO oxidation.

3.1.7 COLLOIDAL MIXING METHOD [1]

The colloidal solution of gold is diluted with isopropyl ether by 50 times, this is followed by the addition of the powder of metal oxide support to make an organic suspension. After stirring for 1h, the organic solvent is vacuum evaporated at 373K for 4h, and the dried Au-metal oxide mixture is then calcined in air at temperatures from 473K to 873K.

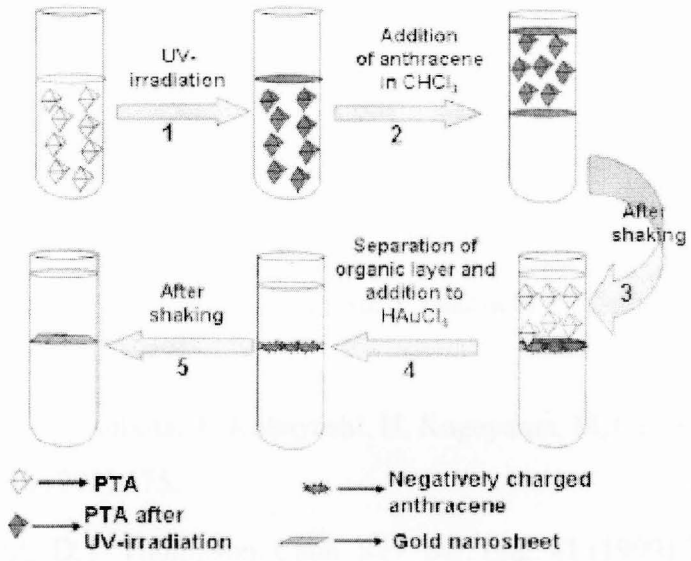


Figure 3.2 Scheme showing the various steps in the synthesis of gold nanosheets at the interface between anthracene-containing chloroform and aqueous chloroauric acid solution [29].

Swami et al [29] investigated another method of synthesizing supported gold nanoparticles in growing them at the air-water interface by the spontaneous reduction of sub-phase chloroaurate ions by 4-hexadecylaniline Langmuir monolayers. They have demonstrated the synthesis of gold nanoparticles of predominantly sheet-like morphology by the reduction of aqueous chloroaurate ions at the interface between aqueous chloroauric acid and chloroform containing anthracene anions as illustrated in Fig. 3.2. Anthracene is the smallest unsubstituted aromatic hydrocarbon with a positive electron affinity (0.53 eV) and can exist in a stable anionic state. They have accomplished electron transfer to anthracene molecules present in chloroform by exposure to photochemically reduced aqueous phosphotungstate [PTA, Keggin ions, (PW12O40)32] ions (step 3, Fig. 3.2) Thereafter, the anthracene anions are exposed to aqueous chloroaurate ions (steps 4 and 5, Fig. 3.2) and lead to the reduction of the metal ions and formation of gold nanosheets at the liquid– liquid interface [30].

3.2 REFERENCES

[1] M. Haruta, Report of the osaka national research institute (ONRI), No. 393 (April 1994-March 1999) pg 7, "The abilities and potential of gold catalyst".

[2] M. Haruta, T. Kobayashi, H. Sano, N.Yamada, Chem. Lett. **405** (1987).

[3] Y. Lizuka, T.Tode, T.Takao, K.Yatsu, T.Takeuchi, S.Tsubota, M. Haruta, J. Catal. **187** (1999) 50.

[4] M. Haruta, S. Tsubota, T. Kobayashi, H. Kageyama, M.J. Genet, B. Delmon, J. Catal. **144** (1993) 175.

[5] G.C. Bond, D.T. Thompson. Catal. Rev. Sci. Eng. **41** (1999) 319.

[6] S. Tsubota, M. Haruta, T. Kobayashi, A. Ueda, Y. Nakahara, in: G. Poncelet, (Eds.), Preparation of Catalysts, vol. V, Elsevier, Amsterdam, (1991) 695.

[7] M. Haruta, S. Tsubota, T. Kobayashi, H. Kageyama, M. Genet, B. Delmon, J. Catal. **144** (1993) 175.

[8] S. Tsubota, D.A. Cunningham, Y. Bando, M. Haruta, in: G. Poncelet, (Eds.), Preparation of Catalysts, vol. VI, Elsevier, Amsterdam, (1995) 227.

[9] M.A. Centeno, M. Paulis, M. Montes, J.A.Odriozola, Appl. Catal. A. **234** (2002) 65.

[10] A.I. Kozlov, A.P. Kozlova, H. Liu, Y. Iwasawa, Appl. Catal. A **182** (1999) 9.

[11] M. Á. Centeno, I. Carrizosa, J. A. Odriozola, Appl. Catal. **246** (2003) 365.

[12] M. Haruta, S. Tsubota, T. Kobayashi, H. Kageyama, M. J. Genet, B. Delmon, J. Catal. **144** (1993) 175.

[13] M. Haruta, Catal. Surveys Japan **61** (1997)1.

[14] http://taylorandfrancis.metapress.com/(vgqbc0m1wqqhg545lxum2q2a)/app/home/contribution.asp?referrer=parent&backto=issue,2,3:journal,25,27:linkingpublicationresults,1:102594,1 30/05/2005.

[15] M. Khoudiakov, M.C. Gupta, S. Deevi, Appl. Catal. A: General **219** (2005) 151.

[16] F.E. Wagner, S. Galvagno, C. Milone, A.M. Visco, L. Stievano, S. Calogero, J. Chem. Soc, Faraday Trans. **93** (1997) 3403.

[17] S. Galvagno, G. Parravano, J. Catal. **55** (1978)178.

[18] S.D. Lin, M. Bollinger, M.A. Vannice, Catal. Lett. **17** (1993) 245.

[19] W.S. Epling, G.B. Hoflund, J.F. Weaver, S. Tsubota, M. Haruta, J. Phys. Chem. **100** (1996) 9929.

[20] M. Haruta, N. Yamada, T. Kobayashi, S. Iijima, J. Catal. **115** (1989) 301.

[21] C. Mohr, P. Claus, Science Progress **84** (2001) 311.

[22] M. Haruta, Cattech **6** (2002) 102.

[23] M. Haruta, Catal. Today **36** (1997) 153.

[24] C. Mohr, H. Hofmeister, M. Lucas, P. Claus, Chemical Engineering Technology **23** (2000) 324.

[25] V. Ponec, G.C. Bond Catalysis by Metals & Alloys, Elservier, Amsterdam, 1996.

[26] D. Guillemot, V.Y. Borovkov,V.B. Kazansky, M. Polisset-Thfoin, J. Fraisard, J. Chem. Soc. Faraday Trans. **93** (1997) 3587.

[27] M. Okamura, S. Nakamura, S. Tsubota, T. Nakamura, M. Haruta, VII International Symposium on Scientific Bases for the preparation of Heterogeneous Catalysts, Studies in Surface Science Catalysis, Elsevier, Amsterdam, **118** (1998) 277.

[28] M. Haruta, J. New. Mat. Electrochem. Systems **7** (2004) 163.

[29] A. Swami, A. Kumar, P.R. Selvakannan, S. Mandal, R Pasricha, M. Sastry, Chem. Mater. **15** (2003) 17.

[30] A. Troupis, A. Hiskia, E. Papaconstantinou, Angew. Chem. Int. Ed. **41** (2002) 1911.

CHAPTER 4

TEMPERATURE-PROGRAMMED ANALYSIS (TPD)

The interaction of the reactant gas with the surface of the catalyst was studied by Temperature-Programmed Desorption (TPD). This Chapter describes TPD and comments on its use in studies of catalysis. The adsorption process is also presented and the basic principles involved e.g. chemisorption and physisorption processes. Basically, the adsorbed carbon oxide is detected by thermal conductivity detector in the TPD system, the desorbing component goes through the methanator with the nickel catalysts and is detected by FID as methane. Methanation is discussed as well in this chapter.

4.1 BACKGROUND

The interaction of reactants with the surface of the catalyst is extremely important in heterogeneous reaction systems [1]. To characterize solid catalysts, some new techniques are utilized. These techniques are: Auger Electron Spectroscopy (AES), X-Ray photoelectron Spectroscopy, (XPS) and Flash Desorption Spectroscopy (FDS). Ultra-high vacuum is usually required to study the mechanism of bonding between the adsorbates and the adsorbing surface. Temperature programmed analysis do not necessarily need vacuum and the adsorbed material can enter into a flow of carrier gas. The concentration of the desorbing particles is recorded as a function of the temperature for a linear increase in temperature. However, this method has been applied over a wide range of temperature-programmed applications like Temperature-Programmed Desorption (TPD), Temperature-Programmed Surface Reduction (TPSR) Temperature-Programmed Oxidation (TPO) and Temperature-Programmed Reactions, for example methanation, sulphidation and carburization [1]. It has been developed further and can be applied to industrial catalysts because it operates under practical conditions. In 1972 [2], Cvetanovic and Amenomiya performed a formal inspection of the application of

temperature-programmed analysis techniques (TPD and TPR) and a study by Falconer and Schwarz dates from 1983 [3, 4]. Bhatia et al. observed that during that time many reviews, typically, solid-gas reactions and the catalyst being supported metal catalyst started to exist. These techniques were developed for characterization of such catalysts.

4.2 APPLICATION

4.2.1 BACKGOUND

Temperature-programmed techniques are importantly used to:

- Analyse supported catalysts by temperature-programmed reduction.
- Determine the activation energy of desorption, binding states of adsorbed molecule (TPD) and surface acidity of zeolites (temperature-programmed deammoniation).
- Measure the metal surface area, dispersion of metal and adsorption kinetics (TPD).
- Study catalytic reactions (temperature-programmed reaction studies).
- Analyse the coke species in deactivated catalysts (TPO).

TPD can be used in identification of active sites in the catalyst surface. Catalytic activity is connected to the number of active sites on the surface. In heterogeneous catalysis, reactions occur on these active sites and thus, the reaction rate depends on the number of the active sites on the catalyst's surface [5]. All the active sites are not identical. Some of the sites are not able to react with adsorbates, or they can have different reaction rates. At steady-state conditions, the reaction rate is proportional to the number of active sites on the macroscopic scale, and the increase in the catalyst's mass also increases the reaction rate with the same magnitude [5].

Equipment for catalyst analysis by temperature-programmed desorption has been reported [5]. Figure 4.1 shows a schematic diagram of TPD apparatus and figure 4.2 shows a picture of such desorption (TPD).

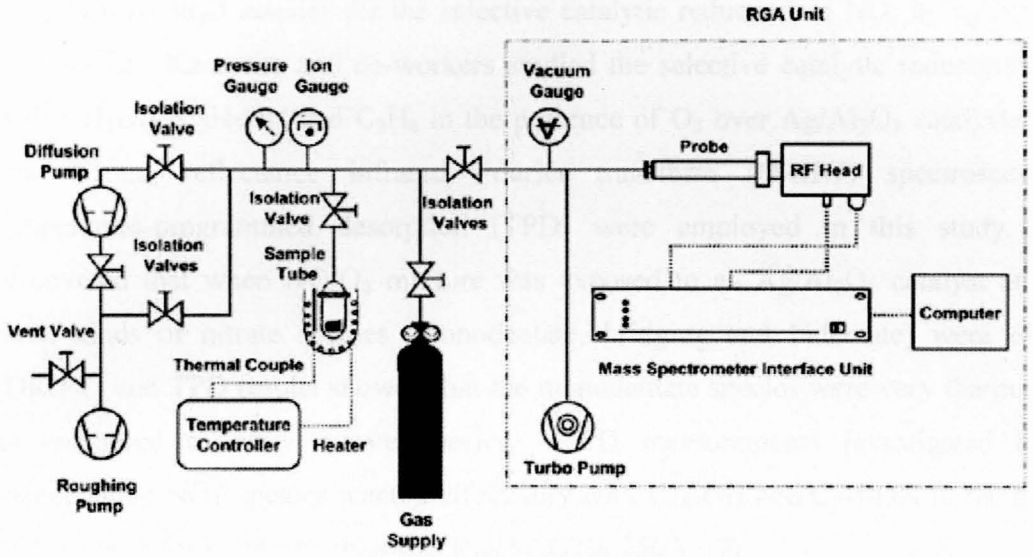


Figure 4.1 Schematic representation of a TPD apparatus [5].

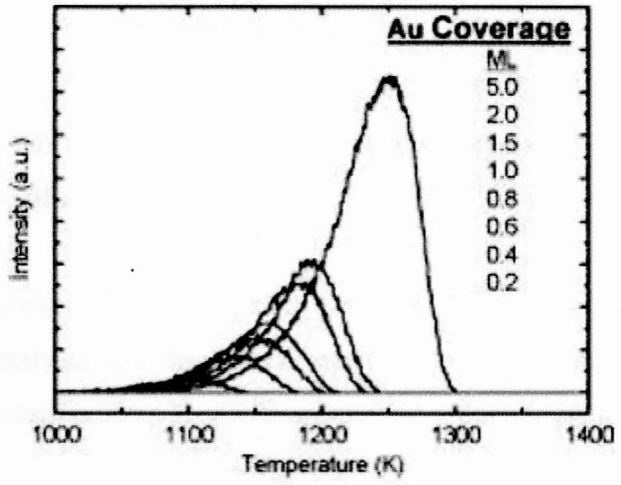


Figure 4.2 A set of TPD spectra of Au (m/e=197) on a 2.5-nm-thick SiO_2 thin film on Mo (110) at Au cluster coverages ranging from 0.2 to 5.0 ML [6]

4.2.2 USES OF TPD AGAINST THE ENVIRONMENTAL POLLUTANTS (NO_x)

Recently, silver catalysts have been investigated as interesting catalysts which perform the relatively high activity for the selective catalytic reduction of NO_x by hydrocarbons (C_3H_6OH,). Kameoka and co-workers studied the selective catalytic reduction of NO_x with CH_3OH, C_2H_5OH and C_3H_6 in the presence of O_2 over Ag/Al_2O_3 catalysts [7]. In situ diffuse reflectance infrared Fourier transform (DRIFT) spectroscopy and temperature-programmed desorption (TPD) were employed in this study. They discovered that when NO/O_2 mixture was exposed to an Ag/Al_2O_3 catalyst at 105°C, three kinds of nitrate species (monodentate, bridging and bidentate) were observed (DRIFT) and TPD results showed that the monodentate species were very thermal stable as compared to other nitrate species. TPD measurements investigated that the monodentate NO_3^- species reacted effectively with CH_3OH and C_2H_5OH in the presence of oxygen to form the adsorbed species (NCO) at 250°C [7].

TPD results investigated that when NO/O_2 mixture was adsorbed on the surface of Ag/Al_2O_3, NO_x species were formed on the surface of these solids and these nitrate species were reduced to N_2 with CH_3OH, C_2H_5OH and C_3H_6, the formation of organic nitrate compounds (NCO) took place in the $NO\text{-}O_2\text{-}C_2H_5OH$ and $NO\text{-}O_2\text{-}C_2H_5OH$ systems even below 300°C [7]. $NO\text{-}O_2\text{-}C_2H_5OH$ system showed high NO_x conversion in the temperature range of 250°C to 400°C.

Tabata and the co-workers [8] also studied the TPD of NO_x and activity measurements for various oxide catalysts and discovered that the strongly bound nitrites and nitrates appeared to be true intermediates in selective catalytic reduction by hydrocarbons.

Therefore, TPD can be used in the reduction of NO_x species which are problems in the environment. It can also help us to understand the mechanism of NO_x reduction to less harmful products (N_2 and O_2).

4.4 EXPERIMENTAL TECHNIQUES

4.4.1 PROCEDURE

In a typical temperature-programmed analysis experiment, a small amount (0.2-0.3g) of catalyst is weighed and placed in a reactor that can be heated by a furnace. The catalyst is heated under temperature-programming conditions in a reducing or oxidizing atmosphere. An appropriate detector such as thermal conductivity detector/mass spectrometer is used to analyse changes in concentrations in the carrier gas [1]. A small thermocouple is inserted inside the heating jacket just next to the reactor to measure any temperature change in a TPD system. The flow rate of the reactant gas has to be noted usually 30 ml /min. does and the heating rate of $10^{o}C$/min. Normally, the catalysts is first calcined at a certain temperature in flowing helium and the temperature of the reactor cooled to adsorption temperature, when adsorption of the reactant gas is complete, the reactor is flushed with helium to remove weakly bound form of the reactant gas and desorption occurs. The outputs are collected from the computer system. Most of temperature programmed analyses are normally run at atmospheric pressure, although higher pressures can be used.

A typical temperature-programmed analysis of catalysts must have the following basic components in the apparatus:

- U-shaped quartz reactor.
- A furnace with programmable temperature controller.
- A dosing system for carrier and adsorbate gases.
- Gas chromatography (GC) or other suitable detectors.
- Vacuum system.

A gas chromatography can be replaced by mass spectrometer so as to obtain direct information about the desorbed molecules [1].
Following are the parameters to be optimized in temperature-programmed analysis:

- The flow rate of a carrier gas.
- Reactant gas/inert gas ratio.
- Catalyst sample volume
- Catalyst sample particle size.
- Geometry of the reaction vessel (catalyst sample reactor).
- Heating rate.
- Signal intensity.
- System pressure.

Steps to be taken into account when using Temperature-programmed desorption:

- Pre-treatment of the catalyst
- Exposure to the adsorbate
- Desorption of the physisorbed fraction by extensive evacuation
- Heating of the catalyst sample using a linear temperature program.
- The desorbed material is transported to the detector by a stream of inert gas usually (He, Ar or N_2) and recorded.
- Characterization of the desorbed material by gas chromatography or by mass spectroscopy.

4.5 THEORY

Temperature-programmed analysis has been used in adsorption, desorption and surface reaction experiments for example TPD has been used to study the binding of adsorbates to catalytic surfaces. The desorption temperature, the shape of the desorption peak and heating rate are all analysed to give information about the binding character the adsorbate/substrate system [9]. Higher peak temperature shows that the adsorbate is more strongly bound to the surface. The number of adsorption sites present in the catalyst plays a major role in the analysis. Kinetic models were developed to account for

the surface heterogeneity [10]. Temperature-programmed desorption traces sometimes shows multiple peaks, implying that, the heats of adsorption on various sites differ significantly. Multiple peaks in a TPD spectrum can be due to lateral interaction between adsorbate molecules (induced heterogeneity) [11] and diffusion of adsorbate in the subsurface region [12]. The determination of reliable kinetic parameters is regarded as too demanding as there is strong possibility of creating experimental errors [1].

The shape and position of the spectra can be influenced by several factors in temperature-programmed analysis, these factors are: surface heterogeneity, readsorption, mass transfer effects, subsurface diffusion and desorption kinetics [1].

4.6 TEMPERATURE-PROGRAMMED DESORPTION (TPD)

4.6.1 BRIEF DESCRIPTION OF THE TECHNIQUE

In a typical temperature programmed desorption (TPD) experiments on supported metal catalyst, about 10 to 300 mg of the catalyst is placed in a reactor that can be heated by a furnace. An inert gas, usually helium at atmospheric pressure, flows over the catalyst. This might be followed by pre-treatment to achieve a reduced catalyst, and then a gas is adsorbed on the surface of the catalyst normally by pulse or continues injection of the adsorbate into the carrier gas upstream from the reactor. The catalyst is heated to create a linear rise in temperature with time. A thermocouple is usually inserted in the catalyst or in the heating jacket to measure any temperature change during the system. A detector measures the change in composition of predominantly inert gas stream. As the catalyst is heated adsorbed gas desorbs or decomposes. A desorption spectrum is a record of the concentration of desorbed gas as a function of temperature. The shape and position of the peak provide information about desorption process and how the gas is adsorbed on the surface of the catalyst.

4.7 ANALYSIS TECHNIQUES

Many techniques have been reported in the literature which can be used to temperature-programmed desorption to determine kinetic parameters. These techniques are applied in the analysis of temperature-programmed desorption depending on the experimental data obtained. The main aim of a TPD experiment is to analyse that data and obtain the mechanistic information and kinetic parameters.

Temperature-Programmed Desorption identifies the strength, the number and the type of active sites that are available on the surface. TPD provides information on heterogeneity of solid catalysts. The desorption temperature, the shape of the desorption peak, the flow rate variation, adsorption temperature and how these affect the surface coverage and surface heterogeneity are analyzed to give information about the binding behaviour of the adsorbate/substrate system [13]. This technique consists of desorbing, by means of a linear temperature increase, a reactive gas previously chemisorbed on the surface [14]. The inert carrier gas carries evolved species from the sample to the detector as the furnace heats the sample. The catalyst is first degassed then sometimes reduced in flowing hydrogen, degassed again and finally saturated with a suitable reactive gas for studies on metals. When the test gas saturates the active sites, a linear temperature increase is applied to the reactor.

An inert carrier gas flows before entering the reactor, and passes through the reference filaments of a thermal conductivity detector (TCD). In the reactor, the inert carrier transports the gas molecules that are adsorbed from the catalyst surface at different temperatures and finally enters the analytical reactor channel. During the desorption process the detector bridge is unbalanced and the electrical signal is collected by the acquisition software [9]. The total amount of gas adsorbed by the sample is obtained by integrating the area under the desorption peaks. The area under the peak is proportional to the amount originally adsorbed, i.e. proportional to the specific adsorption [14].

Knowing the stoichiometry of the gas/solid reaction, one can quantify the total number of active sites that are available on the catalyst surface [14]. One implication of the last point is that if there is more than one binding state for a molecule on a surface then this will normally give rise to multiple peaks in the TPD trace [9]. But multiple peaks are sometimes due to induced heterogeneity. The area under a TPD curve is proportional to the initial coverage of the adsorbate before desorption occurs.

4.8 THE NATURE OF GAS SORPTION AT THE SURFACE

When the interaction between a surface and an adsorbate is relatively weak physisorption takes place. However, surface atoms often possess electrons or electron pairs which are available for chemical bond formation. This irreversible adsorption, or chemisorption, is characterized by large interaction potentials which lead to high heats of adsorption.

4.9 FUNDAMENTAL PRINCIPLES

4.9.1 PHYSISORPTION AND CHEMISORPTION

Adsorption of the reactant gas or the test molecule on the surface of the catalyst is the first step in every reaction in heterogeneous catalysis. Adsorption takes place when an attractive interaction between a particle and a surface is strong enough to overcome the disordering effect of thermal motion. Chemisorption involves a chemical bond between adsorbate and the adsorbent i.e. the molecule interacts chemically with the surface. It is characterized by the activation energy of desorption typically exceeding 50 kJ/mol. When the attractive interaction results from van der Waals forces then physisorption occurs. Physisorption is recognized by activation energies below approximately 50 kJ/mol.

This work suggests that carbon monoxide and carbon dioxide are both physisorbed on 1wt% Au/TiO_2, this was investigated by the activation energy of desorption of 6.0 kJ/mol for both carbon oxides.

It is reported that the chemisorption of carbon monoxide on gold surfaces is generally weak, it cannot lift the reconstruction of the Au(110)(1x2) surface to restore the normal (1x1) phase [15].

4.10 THE PROCESS OF GAS ADSORPTION ON THE SURFACE OF SOLID MATERIAL

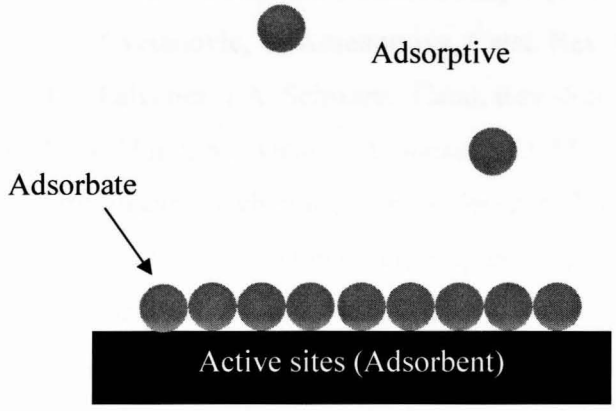


Figure 4.3 Schematic representation of adsorption process.

In this study, the adsorption of carbon monoxide and carbon dioxide on the surface of gold supported catalysts is investigated. The sample was placed in a reactor and was supported with quartz wool, which does not contribute to the whole system. When the gas molecules are inside the reactor but do not interact with the catalyst surface, we call them adsorptive. When there is any interaction with the adsorption sites present in the catalyst surface, the adsorbed gas is the called the adsorbent.

4.11 METHANATION

Methanation has been a subject of many studies and extended reviews because of the importance of its reaction [16,17]. The main concern with this reaction is to remove traces of carbon oxides (CO_2 and CO) into methane with the use of a nickel catalyst.

In this study methanation was used to detect desorbing carbon oxides as methane and FID was used instead of TCD to increase sensitivity by several orders of magnitudes.

4.12 REFERENCES

[1] S. Bhatia, J. Beltramini, Catal. Today **7** (1990) 309.

[2] R.J. Cvetanovic, Y. Amenomiya, Catal. Rev. **6** (1972) 21.

[3] J.L. Falconer, J.A. Schwarz, Catal. Rev.-Sci. Eng. **25** (1983) 141.

[4] N.W. Hurst, S.J. Gentry, A. Jones, B.D. McNicol, Catal. Rev. **24** (1982) 233.

[5] http://userpage.chemie.fu-berlin.de/~pcfp/V18/pdf/v18.pdf 15/02/2005.

[6] http://www.chem.tamu.edu/rgroup/goodman/pdf%20files/421encyclopedia nanosci_tech_04.pdf 20/02/2005.

[7] S. Kameoka, Y. Ukisu, T. Miyadera, Phys.Chem.Chem.Phys. **2** (2000) 367.

[8] M. Tabata, H. Tsuchida, K. Miyamoto, T. Yoshinari, H. Hamada, Y. Kintaichi, M. Sasaki, T. Ito, B: Appl. Catal. **6** (1995) 169.

[9] http://www.chembio.uoguelph.ca/Thomas/oldthom/tpdexpl.htm 15/02/2005.

[10] Y. Tokoro, T. Uchijima, Y. Yoneda, J. Catal. **56** (1979) 110.

[11] J. T. Yates, Methods of experimental physics (R.L. Pard, ed.), **22** (1985), Academic Press: New York.

[12] K.J. Leary, J.N. Michaels, A.M. Stacy, AIChEJ, **34** (1988) 263.

[13] M. Otremba, W. Zajdel, React. Kinet. Catal. Lett. **51** (1993) 473.

[14] http://www.thermo.com/com/cda/resources/resources_detail/1,,13227-10398,00.html. 24/02/2005.

[15] J.M. Gottfried, K.J. Schmidt, S.L.M. Schroeder, K. Christmann, Surf. Sci. **536** (2003) 206.

[16] M. Greyson, P.H. Emmett, Ed. Catalysis, Reinhold: New York.

[17] V.M. Vlasenko, G.E. Yuzefovich, Russ. Chem. Rev. **38** (1969) 729.

CHAPTER 5

EXPERIMENTAL

The reagents as well as the equipments used in this work are discussed. The procedure used to prepare gold supported catalysts, characterization techniques employed in this study are described as well. Temperature-Programmed Desorption has been used in this work to study the binding of the adsorbate to the catalyst surface. Powder X-Ray Diffraction equipment was also used in order to see the effect of gold on the structural properties of titanium dioxide and to attempt to characterize any crystalline gold present. The experimental arrangement used is shown in figure 5.2.

5.1 PREPARATION OF THE CATALYST

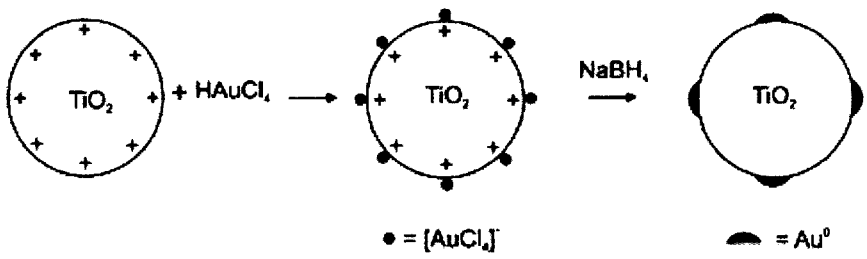


Figure 5.1 Preparation of gold nanoparticles on a metal oxide support by $NaBH_4$ reduction [1].

The catalysts were prepared by the deposition-precipitation method of preparation which involves using a suspension of TiO_2 (Degussa P25) in distilled water (500 ml) under the application of vigorous stirring. A required amount of $HAuCl_4$ (Aldrich 99.99%) solution was added slowly with continuous stirring. The pH of the solution was then maintained at 8.5 by drop-wise addition of 15 % NH_4OH. The precipitated solution was aged for 2h.

A solution of $NaBH_4$ was prepared in ice water, and added in the required amount to ensure that the complete reduction of Au(III) to Au(0) could take place. The colour of the solution turned from white to pink due to the formation of nanosized gold particles on the TiO_2. The suspended solution containing Au^0- TiO_2 was then aged for 4h. After filtration, a colourless filtrate was obtained. This indicates that all gold particles are embedded on the TiO_2. The pink coloured solid mass was dried in an oven at 120°C for 4h. Preparation of gold nanoparticles on a titanium dioxide support by sodium borohydride reduction is shown schematically in figure 5.1 as reported by Scurrell and Kaushik Mallick [1].

5.2 REAGENTS

Titanium dioxide, TiO_2 (P25, Degussa) was chosen as a support, because of its high surface area, porosity, good mechanical properties and relative inertness. It has also been extensively employed as a support for gold catalysts within our research group and by many others. $HAuCl_4$ (Aldrich, 99.99%) was used as a precursor for the Au nanoparticles. $NaBH_4$ (Fluka) was used (in excess) for reduction of Au^{3+}, 15 % NH_4OH (Aldrich) was used in maintaining the pH of the solution at 8.5 [1]. 10 % CO in helium, 99.9% CO_2, air, 99.999 % hydrogen, 99.999% helium cylinders were obtained from Afrox. The chemicals were used as received with out any further analysis and purification. The intended gold loading was 1.0wt %, 2wt% and 3wt%. In some cases the gold content was determined by means of fire assay with fining using atomic absorption spectroscopy. The methanator with the nickel catalyst was obtained from CHROM Tech Incl. at USA.

5.3 METHOD OF ANALYSIS

5.3.1 CHARACTERIZATION OF THE CATALYST

The catalysts were characterized using Temperature-Programmed Desorption (TPD) and Powder X-Ray diffraction.

5.3.1.1 Temperature-Programmed Desorption (TPD) apparatus

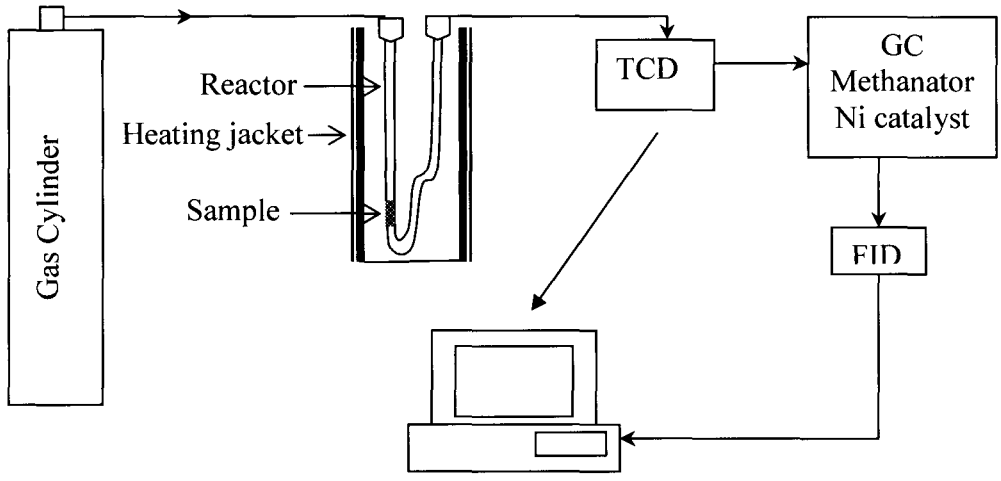


Figure 5.2 Schematic diagram of TPD apparatus.

In a typical temperature-programmed analysis experiment, a small amount (0.25g) of the sample (Au/TiO_2 or TiO_2) was weighed and placed in a U-shaped micro quartz reactor. The catalyst samples rested on quartz wool were calcined in helium flowing at 30 ml/min for 1h. After that, the reactor was cooled to room temperature in flowing helium. A mixture of acetone and liquid nitrogen was prepared and the reactor was immersed in the cold bath (-80°C). Carbon monoxide or carbon dioxide was adsorbed on the surface of these solids at 30 ml/min. (unless otherwise stated) for 30 min. After adsorption, the reactor was flushed with helium to remove weakly bound form of carbon oxide, the cold bath was removed from the reactor and the TPD programme was started. Both thermal

conductivity detector and FID were used to analyse changes in concentrations in the carrier gas. A small thermocouple was placed just next to the reactor to measure any temperature change in a TPD system. Temperature increased from adsorption temperature (-80°C) to room temperature by natural warming. The outputs were collected from the computer system.

The TPD experiments were carried out with and without the methanator. The same procedure as above was used for methanation but the catalyst samples were calcined in pure hydrogen under the same conditions.

The methanator with the nickel catalyst was connected to the system to increase the sensitivity. When the TPD experiments were carried out without the methanator, carbon monoxide or carbon dioxide was adsorbed on the surface of the solid, the desorbing species were detected by TCD and the outputs were collected from the computer system.

When the methanator was used, carbon monoxide or carbon dioxide was adsorbed on the surface of the solid material, the desorbing species were detected by TCD. Whatever is being detected by TCD passed through the methanator with the nickel catalyst which is used for the hydrogenation of carbon oxides. The methane formed was detected by FID and the outputs were collected from the computer system.

When the methanator was bypassed, no signal was recorded by FID demonstrating that no methane was formed by direct interaction of hydrogen with the adsorbed CO and/or CO_2. All methane detected was produced only by the methanator.

At first, the thermocouple was calibrated, a mixture of acetone and liquid nitrogen was prepared and the thermocouple was immersed in the mixture. The computer system was programmed to record any change in the output (mV) with the thermocouple temperature.

Carbon monoxide or carbon dioxide was also adsorbed at room temperature on the surface of Au/TiO_2 or TiO_2. In this case the catalyst samples were calcined at 400°C for 1h in helium (hydrogen for methanation) at 30 ml/min. After calcination, the reactor was cooled to room temperature in flowing helium or hydrogen. Carbon monoxide or carbon dioxide was adsorbed at room temperature for 30 min. at 30 ml/min. unless otherwise stated. After adsorption the reactor was flushed with the carrier gas to remove weakly bound CO or CO_2. A small thermocouple was inserted inside the heating jacket just next to the reactor to measure any temperature change in a TPD system. The catalyst was heated in helium flowing at 30 ml/min. (hydrogen for methanation) from room temperature to 800°C under temperature-programming conditions at 10°C/min. unless otherwise stated. The outputs were collected from the computer system.

For several experiments, the flow rates of the adsorbate, adsorption temperature, heating rate and calcination temperature were varied and a significant effect on the desorption curves was observed. The activation energy of desorption was obtained in some cases. The amount of the desorbing gas was obtained by integrating the area under the desorption peaks and calibrating the TCD and/or FID. Calibration was done by injecting known CO or CO_2 volumes into an empty reactor with flowing helium using a syringe. Area was determined from the desorption curves and a plot of area under the desorption curves against the volume of the adsorbate (CO/CO_2) was drawn and the graph was a straight line. To find the volumes of CO or CO_2 desorbing from the surface of the sample, the area under each desorption curve was determined and either extrapolation or interpolation was employed to determine the volume of CO or CO_2 under the desorption curves. The temperature of desorption is taken as the measure of the adsorption site strength and the area under the desorption peak as a measure of the amount desorbed.

A typical temperature-programmed analysis of the catalysts used in this work has the following basic components in the apparatus:

- U-shaped quartz reactor, quartz wool
- A furnace with programmable temperature controller.

- Gas chromatography (GC), TCD and flame ionisation detector (FID).
- Methanator
- The computer system for outputs

5.3.1.2 Powder X-Ray Diffraction (PXRD)

Approximately 0.5g of Au/TiO_2 or TiO_2 composite material was used for the analysis by powder X-ray diffraction (PXRD). Results were obtained from the advanced D8 Bruker X-ray diffractometer and the conditions of analysis were as follows:

Voltage	: 40 kV
Divergence slit	: 0.6 mm
Receiver slit	: 3°
Scan from	: 5°2θ
Scan to	: 90°2θ
Step size	: 0.02°2θ
Time taken by each scan	: 10 min.
Type of scan	: Mediumres

5.6 REFERENCES

[1] K. Mallick, M.S. Scurrell, Appl. Catal. A **253** (2003) 527.

CHAPTER 6

6.1 MOTIVATION FOR THE STUDY

Adsorption studies of CO on Au/TiO_2 at very low temperature have been carried out and CO was found to desorb very readily from Au/TiO_2 before ca. $-5^{o}C$. Comparative studies were also carried out with CO_2 as the adsorbate. A limited number of adsorption studies of CO_2 have also been carried out on Au supported on TiO_2 in order to investigate the catalytic activity of gold on these supports for potential industrial use. Adsorption of CO on TiO_2 without gold being present is also performed.

6.2 OVERALL AIM AND OBJECTIVES

The overall aim of this project is:

(a) To build and evaluate a TPD apparatus sufficiently sensitive for the measurement of desorption profiles for CO and CO_2 adsorption on Au/TiO_2.

(b) To prepare supported gold catalysts with different gold loading and evaluate their behaviour in the adsorption of CO at room temperature using Temperature-Programmed Desorption (TPD).

(c) To observe the effect of calcination temperature of the catalyst on the adsorption of CO.

(d) To attempt to identify adsorption of CO and/or CO_2 specifically on Au in the TiO_2 supported samples.

(e) To investigate the amount of CO/CO_2 (ml) adsorbed/desorbed and to determine the moles of CO_2 or CO/g catalyst.

CHAPTER 7

RESULTS AND DISCUSSION

The results obtained from the interaction of the adsorbed gas with the surface of the solid material using temperature-programmed desorption (TPD) are reported and discussed in this chapter. Also reported are the results of carbon monoxide and carbon dioxide adsorption on gold supported on titanium dioxide. Calculations of the number of molecules of carbon oxide/g of the Au/TiO_2 composite material are indicated also. The effect of adsorption temperature, heating rate, flow rate and calcination temperature on TPD experiments are shown and discussed. In this study, gold supported on titanium dioxide was analysed by temperature-programmed desorption which is simple and inexpensive. Powder X-Ray Diffraction equipment was also used in order to see the effect of gold on the structural properties of titanium dioxide and to attempt to characterize any crystalline gold present.

7.1 ADSORPTION OF CARBON MONOXIDE ON TiO_2 OR Au/TiO_2

7.1.1 EFFECT OF GOLD ON SURFACE HETEROGENEITY

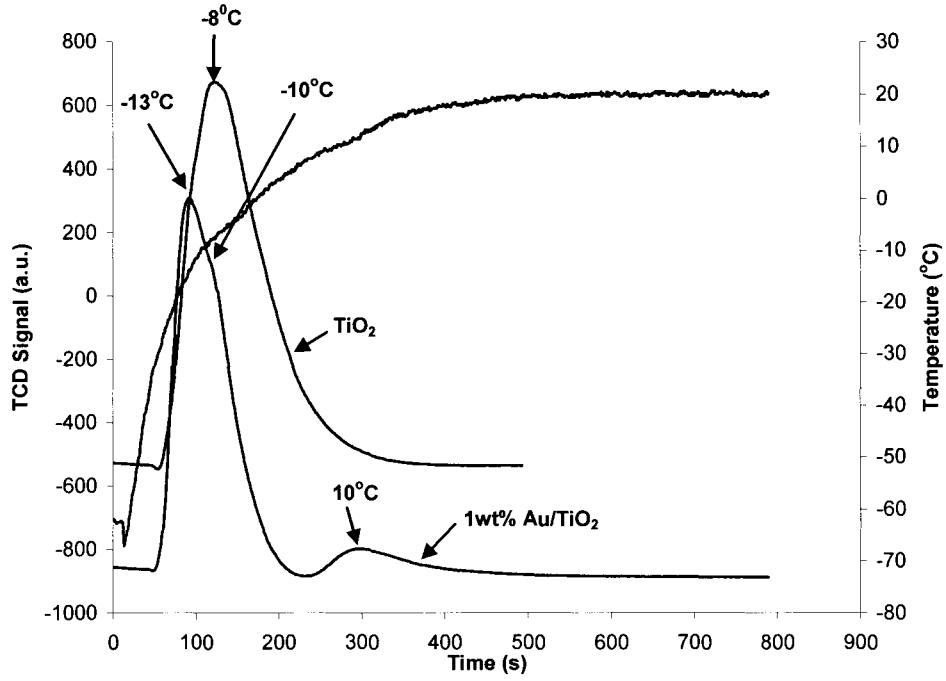


Figure 7.1 Carbon monoxide desorption curves. Both TiO_2 and 1wt% Au/TiO_2 were calcined at 400°C for 1h in helium and cooled in helium before adsorption. Carbon monoxide was adsorbed at -80°C for 30 min. at 30 ml/min. Desorption was carried out from -80°C to room temperature.

Initial tests were run in order to study the effect of gold as revealed by TPD experiments (figure 7.1). When the sample was changed from titanium dioxide to gold on titanium dioxide, three desorption peaks were observed. TPD experiments showed three desorption peaks with peak temperature maxima of -13°C (CO desorption from TiO_2 adsorption sites), -10°C (CO desorption assumed to be from gold sites which are exposed at the contact perimeter between gold particles and the oxide support) and 10°C (weakly adsorbed CO from gold particles). Because carbon monoxide adsorbed at the defects sites of gold is more resistant to desorption [1], higher energy is expected to be required to activate the desorption process and it is unlikely that the desorption seen in figure 7.1 can be explained on this basis. The low temperature peak (-13°C) corresponds to

physically adsorbed carbon monoxide desorbing from titanium dioxide adsorption sites. The desorption peak at -10°C is due to carbon monoxide desorbing from perimeter gold sites. Higher temperature peak at 10°C is due to weakly adsorbed carbon monoxide from gold particles. The total volume of carbon monoxide adsorbed on TiO_2 alone is 2.4 ml with the surface coverage of 2.0×10^{20} CO molecules/g TiO_2. The volume of carbon monoxide desorbing from the same type of adsorption sites is 2.5 ml (essentially unchanged) with the surface coverage of 2.1×10^{20} CO molecules/g 1wt% Au/TiO_2. A significant volume of carbon monoxide adsorption on titanium dioxide adsorption sites was observed, and the amount of carbon monoxide adsorbed on gold particles was found to be very low. Carbon monoxide desorbed in three distinct peaks (from Au/TiO_2) with desorption continuing at slightly higher temperature.

Table 7.1 Specific adsorption for 1wt% Au/TiO_2 and TiO_2 calcined at 400°C in helium for 1h, CO was adsorbed at -80°C for 30 min. at 30 ml/min. Desorption was carried out from -80°C to room temperature.

Sample	Sites	Specific adsorption (molecules/g)	Volume of CO Adsorbed (ml)	Desorption temperature maxima (°C)
TiO_2	[a]TiO_2	2.0×10^{20}	2.4	-8
Au/TiO_2	[a]TiO_2	2.1×10^{20}	2.5	-13
Au/TiO_2	[b]Au/TiO_2	1.8×10^{20}	2.0	-10
Au/TiO_2	[c]Au	4.9×10^{18}	0.059	10

[a]TiO_2 = CO desorption from TiO_2 adsorption sites.

[b]Au/TiO_2 = CO desorption assumed to be from gold sites which are exposed at the contact perimeter between gold particles and the oxide support.

[c]Au = CO desorption from gold particles.

7.1.2 EFFECT OF ADSORPTION TEMPERATURE ON Au/TiO_2

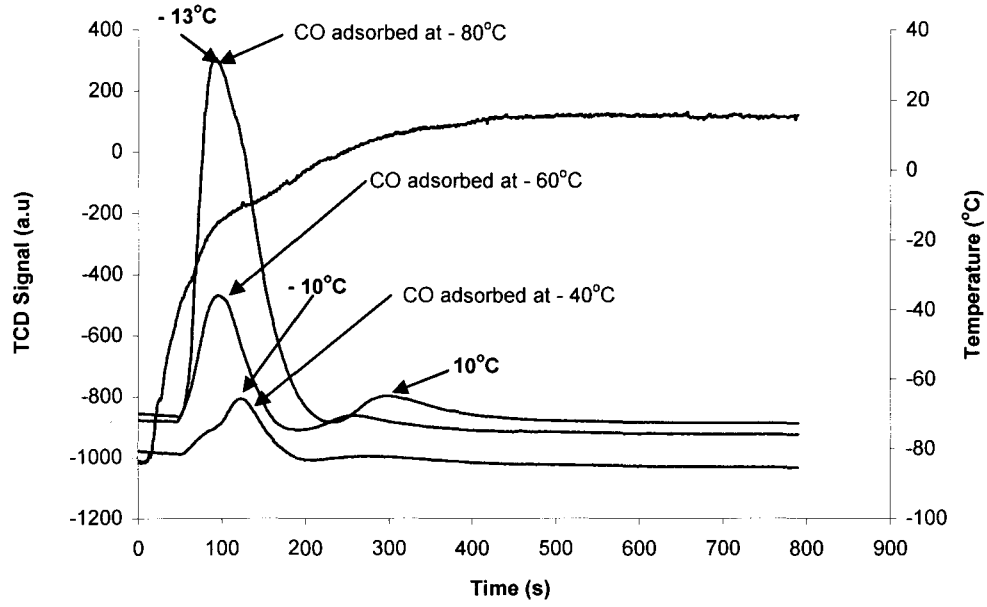


Figure 7.2 Comparison of carbon monoxide desorption from 1wt% gold nanoparticles deposited on TiO_2 showing that there is a significantly higher amount of carbon monoxide adsorbed at -80°C (adsorption temperature) than at other temperatures (-60 & -40°C). Carbon monoxide was adsorbed at 30 ml/min. for 30 min. at different temperatures. All Au/TiO_2 composite materials were calcined at 400°C in helium for 1h and desorption was carried out from adsorption temperature (-80°C, -60°C & -40°C) to room temperature.

The volume of the adsorbate was determined by integrating the area under the desorption peaks. The desorption experiments were carried out on 1wt% Au/TiO_2 samples and figure 7.2 illustrates the effect of carbon monoxide adsorption temperature on the TPD experiments.

When carbon monoxide is adsorbed at -80°C, a significant amount of carbon monoxide (2.5 ml) desorbed from the support and from the perimeter gold sites. The number of carbon monoxide adsorption sites present in the sample does depend on the temperature

in which the adsorbate is adsorbed hence the results differ with adsorption temperature variation. Adsorption of carbon monoxide at -40°C reduces carbon monoxide adsorption on gold particles. Table 7.2 demonstrates the summary of the volume of carbon monoxide adsorbed at different adsorption temperatures. As the adsorption temperature decreased from -40 to -80 °C, the intensity of the desorption curves increased and there is no significant shift in peak temperatures, only the total volume of the adsorbate was affected by adsorption temperature variation. Also listed in table 7.2 is the specific adsorption calculated from the desorption results. This suggests that large amount of CO is adsorbed at very low temperatures (e.g. -80°C) than at higher temperatures.

The volume of the desorbing carbon monoxide from gold site which is exposed at the contact perimeter of the oxide support is also strongly affected by the change in adsorption temperature (fig.7.2). When the CO adsorption temperature is -60°C, the volume of the adsorbate desorbing from the gold site which is exposed at the contact perimeter of the oxide support is very insignificant. The observed increase in the volume of CO adsorbed with a decrease in the adsorption temperature is a result of the formation of multilayers. The adsorption temperature does not change the intrinsic properties of the catalyst, such as % dispersion or metal surface area.

Table 7.2 Specific adsorption for 1wt% Au/TiO_2 calcined at 400°C in helium for 1h, carbon monoxide was adsorbed at different temperatures (-80°C, -60°C and -40°C) at the same flow rate 30 ml/min. for 30 minutes. Desorption was carried out from adsorption temperature (-80°C, -60°C & -40°C) to room temperature.

Sample	Adsorption temperature °C	Specific adsorption (molecules/g)	Volume of CO Adsorbed (ml)	Sites	Desorption temperature maxima (°C)
Au/TiO_2	- 80	2.1×10^{20}	2.5	[a]TiO_2	-13
Au/TiO_2	- 80	1.8×10^{20}	2.0	[b]Au/TiO_2	-10
Au/TiO_2	- 80	4.9×10^{18}	0.059	[c]Au	10
Au/TiO_2	- 60	6.9×10^{19}	0.82	[a]TiO_2	-13
Au/TiO_2	- 60	4.3×10^{18}	0.052	[c]Au	8
Au/TiO_2	- 40	4.9×10^{18}	0.060	[a]TiO_2	-13
Au/TiO_2	- 40	3.2×10^{19}	0.38	[b]Au/TiO_2	-10

[a]TiO_2 = CO desorption from TiO_2 adsorption sites.

[b]Au/TiO_2 = CO desorption assumed to be from gold sites which are exposed at the contact perimeter between gold particles and the oxide support.

[c]Au = CO desorption from gold particles.

7.2 ADSORPTION OF CARBON DIOXIDE ON TiO_2 OR Au/TiO_2

7.2.1 CARBON DIOXIDE ADSORPTION ON TiO_2

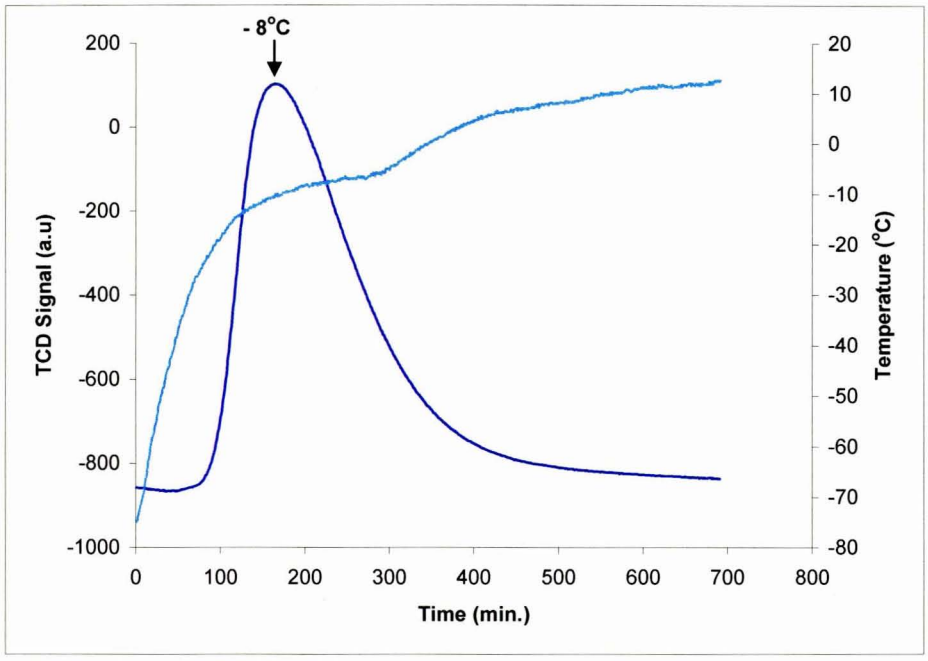


Figure 7.3 Carbon dioxide desorption curve. Carbon dioxide was adsorbed at -80°C on TiO_2 for 30 min. at 30 ml/min. Titanium dioxide was calcined in helium at 400°C for 1hour, cooled in helium to room temperature, this was followed by adsorption at -80°C. Desorption was carried out from -80°C to room temperature.

A typical carbon dioxide desorption curve from a sample of TiO_2 is shown in figure 7.3. From the desorption curve, we find that carbon dioxide desorbs as a single asymmetric peak from titanium dioxide adsorption sites. The desorption temperature maximum is

-8°C. The volume of CO_2 desorbing from the support was found to be 16.8 ml.

7.2.2 CARBON DIOXIDE ADSORPTION ON Au/TiO_2

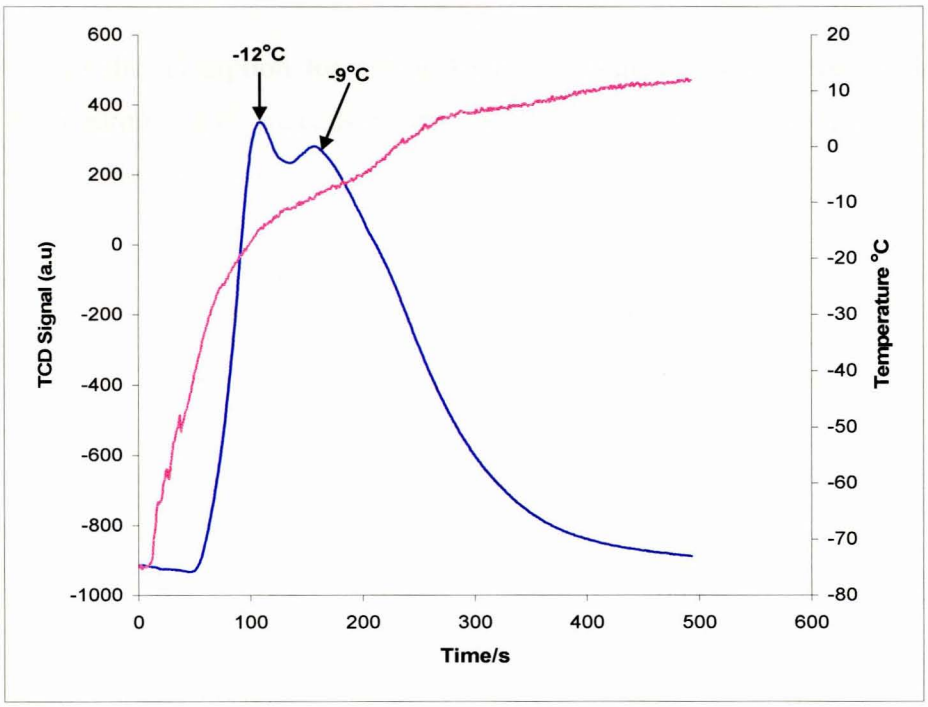


Figure 7.4 Carbon dioxide desorption curve. Carbon dioxide was adsorbed at -80°C for 30 min. at 30 ml/min. on 1wt% Au/TiO_2. Au/TiO_2 composite material was calcined at 400°C for 1hour in helium. Desorption was carried out from -80°C to room temperature.

When 1wt% Au/TiO_2 was exposed to CO_2 at -80°C, a partially resolved doublet was observed. The adsorbed carbon dioxide desorbed from both titanium dioxide adsorption sites and perimeter gold sites (assumption). It was consistent that when CO_2 is adsorbed on Au/TiO_2 samples, the partially resolved doublet is observed. Gold increased the number of adsorption sites as indicated by the doublet shown in (figure 7.4). The TPD results show that there is significant amount of the desorbing carbon dioxide from both

the support and from the perimeter gold sites. The deposition of gold nanoparticles on titanium dioxide resulted in reduced amount (12.8ml) of the desorbing carbon dioxide from the support (figure 7.4) as compared to CO_2 desorbing from the support alone (16.8 ml). Also noted on the TPD curve (figure 7.4) is that there is no desorption peak (at 10°C) attributed to gold particles. Unlike with CO (figure 7.1), the desorption peak at 10°C was observed which is due to gold particles.

Table 7.3 Specific adsorption for 1wt% Au/TiO_2 calcined at 400°C for 1h in helium flowing at 30 ml/min. CO_2 was adsorbed at -80°C for 30 min. at 30 ml/min. Desorption was carried out from -80°C to room temperature.

Sample	Desorption temperature maxima (°C)	Specific adsorption (molecules/g)	Volume of CO_2 Adsorbed (ml)	Sites
Au/TiO_2	-12	1.0×10^{21}	12.8	[a]TiO_2
Au/TiO_2	-9	1.2×10^{21}	14.2	[b]$AuTiO_2$

[a]TiO_2 = CO_2 desorption from TiO_2 adsorption sites.

[b]Au/TiO_2 = CO_2 desorption assumed to be from gold sites which are exposed at the contact perimeter between gold particles and the oxide support.

7.3 METHANATION

7.3.1 ADSORPTION OF CARBON MONOXIDE ON Au/TiO_2 or TiO_2

7.3.1.1 Adsorption of CO on Au/TiO_2 when the methanator is bypassed

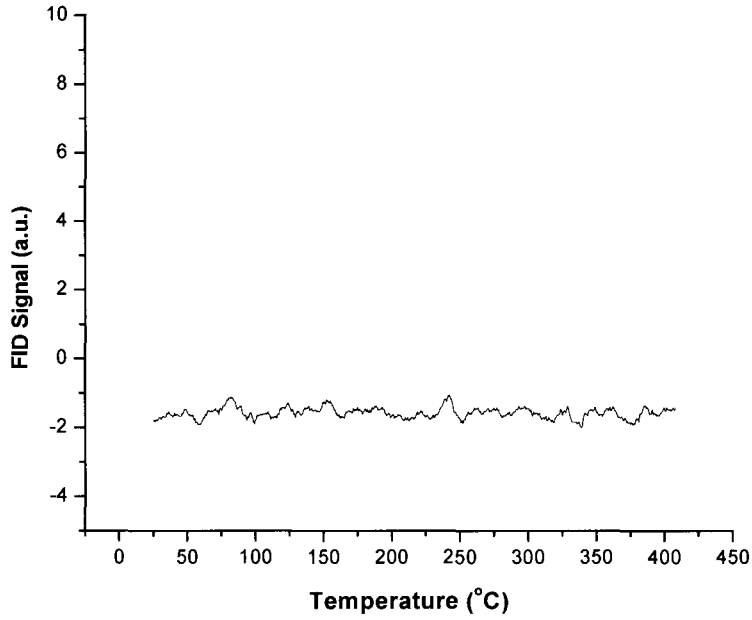


Figure 7.5 Carbon monoxide desorption curve when the methanator was bypassed. 1wt% Au/TiO_2 was calcined at 400°C for 1h in hydrogen. Desorption was carried out from room temperature to 400°C at the heating rate of 10°C/min.

This experiment was done to investigate whether methane forms in the reactor, as hydrogen was used as the carrier gas for calcination. The thermal conductivity detector detects the adsorbed carbon oxide as carbon oxide which goes through the methanator (with the nickel catalyst) and is detected by FID as methane. There is no methane desorption peak detected. So, we can draw the conclusion that no methane formed in the system apart from that formed in the methanator and subsequently detected by FID.

The methanator was used in this work to quantify the results by converting all CO/CO_2 traces into methane. This was done in order to investigate the exact amount of the adsorbate desorbing from the surface of the Au/TiO_2 composite material. All carbon oxides desorbed are being converted to methane and the specific adsorption was determined from these results.

Several experiments were carried out to determine the number of molecules of CO or CO_2/g 1wt% Au/TiO_2 composite material, to study the effect of heating rate, flow rate and the effect of gold on TPD experiments.

7.3.1.2 Adsorption of carbon monoxide on TiO_2

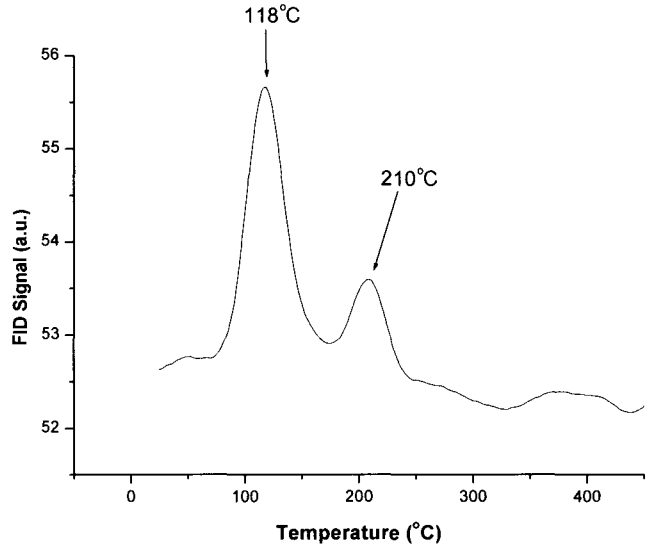


Figure 7.6 Carbon monoxide desorption curve from TiO_2, TiO_2 was calcined at 400°C for 1h in hydrogen, the reactor was cooled to room temperature in flowing hydrogen, carbon monoxide was adsorbed at room temperature for 30 min. at 30 ml/min. Desorption was carried out from room temperature to 500°C at 10°C/min. Desorbed CO was detected as methane.

A typical carbon monoxide desorption curve from a sample of TiO_2 is shown in figure 7.6. From the desorption curve, we see that carbon monoxide desorbs as two distinct peaks from titanium dioxide adsorption sites and these peaks continue to slightly higher temperature. Carbon monoxide desorption temperature maxima from titanium dioxide are 118°C and 210°C respectively. A full interpretation of the TPD data is not possible based on this work alone because there was no mass spectrometry connected to the TPD set up. Some or all of the species desorbing may be connected with the formation of carbonate species.

Table 7.4 Specific adsorption for TiO_2 calcined at 400°C for 1h. Carbon monoxide was adsorbed at room temperature for 30 min. at 30 ml/min. Desorption was carried out from room temperature to 500°C at 10°C/min.

Sample	Specific adsorption (molecules/g)	Volume of CO Adsorbed (ml)	Sites	Desorption temperature maxima (°C)
TiO_2	1.3×10^{19}	0.16	$^{a}TiO_2$	118
TiO_2	3.7×10^{18}	0.045	$^{a}TiO_2$	210

$^{a}TiO_2$ = CO desorption from TiO_2 adsorption sites.

7.3.1.3 Adsorption of CO on TiO_2 or Au/TiO_2

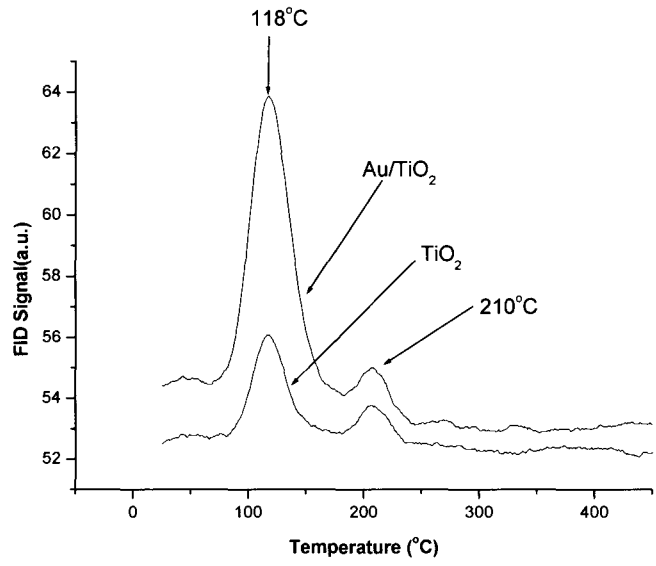


Figure 7.7 Shows the difference between the desorption of carbon monoxide when the sample is changed from TiO_2 to 1wt% Au/TiO_2. Both samples were calcined at 400°C in hydrogen for 1h. Carbon monoxide was adsorbed at room temperature for 30 min. at 30 ml/min. Desorption was carried out from room temperature to 500°C at 10°C/min. Desorbed CO was detected as methane.

The adsorbed carbon monoxide desorbs as two distinct peaks from both TiO_2 and Au/TiO_2. From carbon monoxide desorption curve (figure 7.7), it is shown that gold increases the amount of the desorbing component from the support (TiO_2). There is no desorption peak attributed to gold but specific adsorption (molecules/g) increases due to gold (Table 7.5).

Table 7.5 Specific adsorption for TiO_2 and 1wt% Au/TiO_2. Both samples were calcined in hydrogen at 400°C for 1h. Carbon monoxide was adsorbed at room temperature for 30 min. at 30 ml/min. Desorption occurred from room temperature to 500°C at 10°C/min.

Sample	Specific adsorption (molecules/g)	Volume of CO Adsorbed (ml)	Sites	Desorption temperature maxima (°C)
TiO_2	1.3×10^{19}	0.16	$^aTiO_2$	118
TiO_2	3.7×10^{18}	0.045	$^aTiO_2$	210
Au/TiO_2	4.0×10^{19}	0.48	$^aTiO_2$	118
Au/TiO_2	5.0×10^{18}	0.060	$^aTiO_2$	210

$^aTiO_2$ = CO desorption from TiO_2 adsorption sites.

7.3.1.4 Adsorption of CO on 1wt%Au/TiO_2 at room temperature

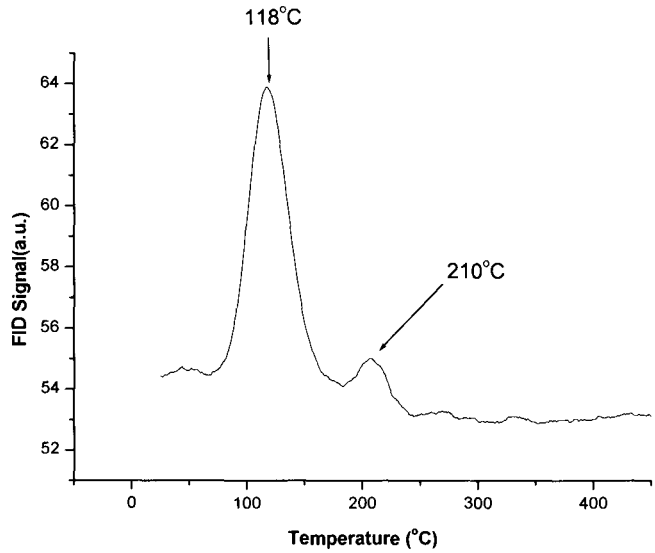


Figure 7.8 Carbon monoxide desorption curve, 1wt% Au/TiO_2 was calcined at 400°C for 1h in hydrogen, CO was adsorbed at room temperature for 30 min. at 30 ml/min. Desorption was carried out from room temperature to 500°C at a heating rate of 10°C /min. Desorbed carbon monoxide was detected as methane.

When carbon monoxide was adsorbed at room temperature, the TPD results showed a very sharp peak at 118°C, which we claim is due to carbon oxide desorbing from titanium dioxide adsorption sites. The second desorption peak at 210°C is also due to carbon oxide desorbing from titanium dioxide adsorption sites. This peak is also observed on titanium dioxide alone (refer to figure 7.6).

Table 7.6 Specific adsorption for 1wt% Au/TiO_2 calcined at 400°C for 1h. Carbon monoxide was adsorbed at room temperature for 30 min. at 30 ml/min. Desorption was carried out from room temperature to 500°C at 10°C/min.

Sample	Specific adsorption (molecules/g)	Volume of CO Adsorbed (ml)	Sites	Desorption temperature maxima (°C)
Au/TiO_2	4.0×10^{19}	0.48	$^{a}TiO_2$	118
Au/TiO_2	5.0×10^{18}	0.060	$^{a}TiO_2$	210

$^{a}TiO_2$ = CO desorption from TiO_2 adsorption sites.

7.3.1.5 Adsorption of CO on 1wt%Au/TiO_2 at -80°C

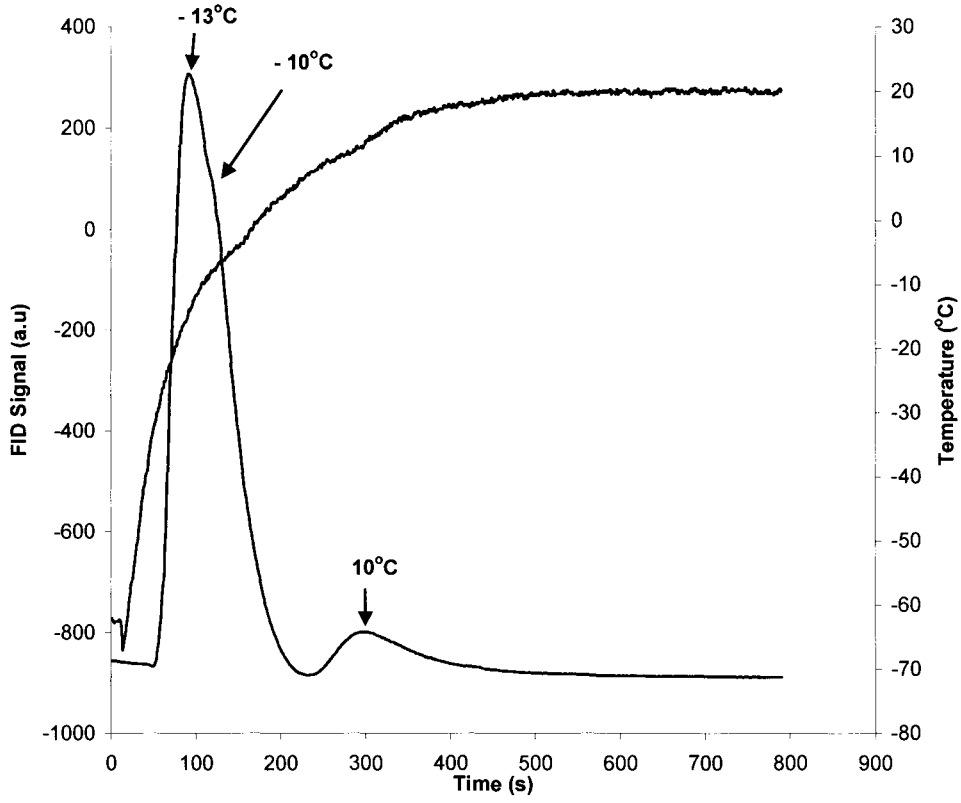


Figure 7.9 Carbon monoxide desorption curve, showing the effect of Au on TPD experiments. CO was adsorbed at -80°C for 30 min. at 30 ml/min. on 1wt% Au/TiO_2 which was calcined at 400°C for 1h in hydrogen. Desorption was carried out from -80°C to room temperature. Desorbed carbon monoxide was detected as methane.

Figure 7.8 (adsorption temperature = room temperature) and figure 7.9 (adsorption temperature = -80°C) are both carbon monoxide desorption curves, showing the difference between carbon monoxide adsorbed at different temperatures. It can be seen clearly that there is little amount (table 7.6) of carbon monoxide adsorbed at room temperature than the volume of this gas adsorbed at -80°C (table 7.7).

Table 7.7 Specific adsorption for 1wt% Au/TiO_2 calcined at 400°C for 1h. Carbon monoxide was adsorbed at -80°C for 30 min. at 30 ml/min. Desorption was carried out from -80°C to room temperature. Desorbed CO was detected as methane.

Sample	Specific adsorption (molecules/g)	Volume of CO Adsorbed (ml)	Sites	Desorption temperature maxima (°C)
Au/TiO_2	2.1×10^{20}	2.5	[a]TiO_2	-13
Au/TiO_2	1.8×10^{20}	2.0	[b]Au/TiO_2	-10
Au/TiO_2	4.9×10^{18}	0.06	[c]Au	10

[a]TiO_2 = CO desorption from TiO_2 adsorption sites.

[b]Au/TiO_2 = CO desorption assumed to be from gold sites which are exposed at the contact perimeter between gold particles and the oxide support.

[c]Au = CO desorption from gold particles.

7.3.1.6 Effect of heating rate

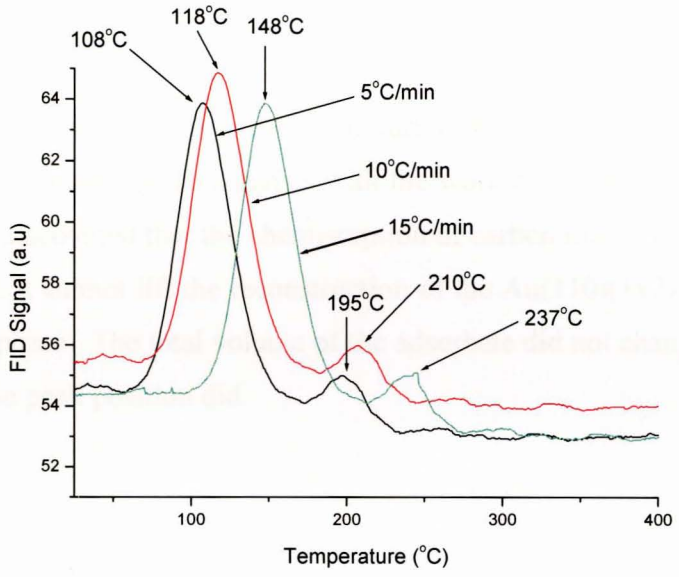


Figure 7.10 Carbon monoxide desorption curves. 1wt% Au/TiO_2 samples were calcined in hydrogen at 400°C for 1h. Carbon monoxide was adsorbed at room temperature for 30 min. at 30ml/min. Desorption occurred from room temperature to 400°C at the heating rate of 15°C/min, 10°C/min. and 5°C/min. Desorbed CO was detected as methane.

Desorption is a thermal activation process, a lager heating rate (h.r.) corresponds to a higher temperature (T_m) at which the maximum intensity occurs, while the intensity can be considered as desorption rates during TPD heating. In this study, the desorption activation energy (E_d) was determined from these TPD results. The relationship between T_m and E_d for a uniform surface is expressed in the following relationship [2].

$$\ln (T^2_m/h.r.) = E_d/R\ T_m$$

Where: R is universal gas constant.

T_m is higher temperature at which maximum intensity occurs and is measured at heating rate (h.r.) between 5 and 15 °C/min.

E_d (activation energy of desorption) is determined from the slope of plot of $\ln (T^2_m/h.r.)$ against $1/T_m$.

h.r. is the heating rate in °C/min.

From the slope of the line, activation energy of 6.0 kJ/mol is obtained (figure 7.11). This low value of activation energy indicates that carbon monoxide is weakly adsorbed on 1wt% Au/TiO_2 solid material. This agrees with the work done by Schroeder and the co-workers [2], they discovered that the chemisorption of carbon monoxide on gold surfaces is generally weak, it cannot lift the reconstruction of the Au(110)(1x2) surface to restore the normal (1x1) phase. The total volume of the adsorbate did not change that much with heating rate but the peak position did.

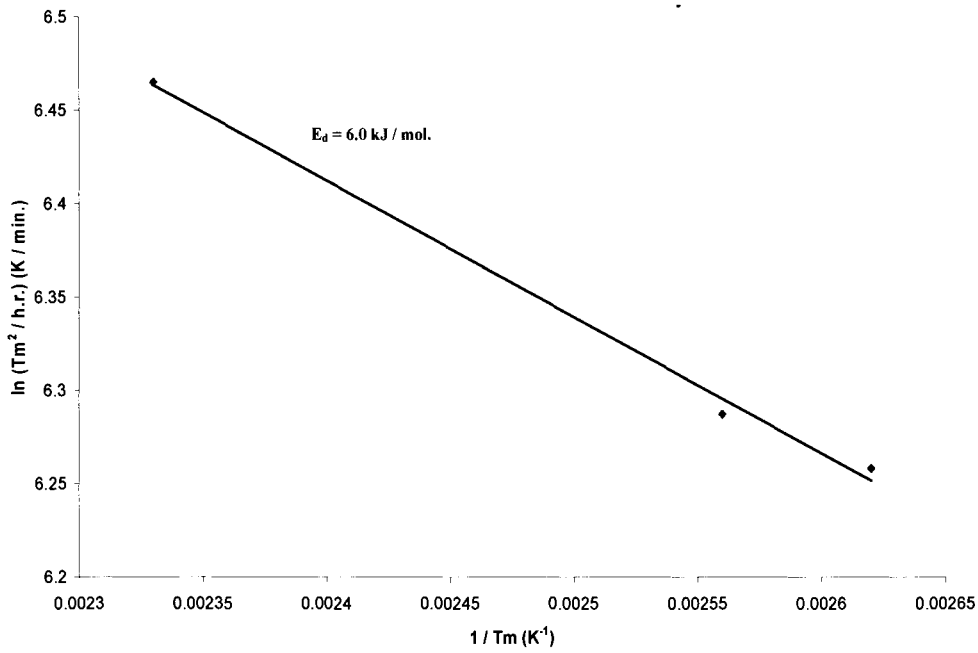


Figure 7.11 Activation energy determination from heating rate variation, ln (Tm^2/h.r.) against $1/T_m$ (K^{-1}) for carbon monoxide.

Table 7.8 Specific adsorption for 1wt% Au/TiO_2 calcined at 400°C for 1h in hydrogen. Carbon monoxide was adsorbed at room temperature for 30 min. at 30 ml/min. Desorption was carried out from room temperature to 400°C at different heating rates (15°C/min, 10°C/min. and 5°C/min).

Sample	Heating rate °C/min.	Specific adsorption (molecules/g)	Volume of CO Adsorbed (ml)	Sites	Desorption temperature maxima (°C)
Au/TiO_2	5	4.0×10^{19}	0.48	$^aTiO_2$	108
Au/TiO_2	5	4.7×10^{18}	0.056	$^aTiO_2$	195
Au/TiO_2	10	4.0×10^{19}	0.48	$^aTiO_2$	118
Au/TiO_2	10	5.0×10^{18}	0.060	$^aTiO_2$	210
Au/TiO_2	15	4.0×10^{19}	0.48	$^aTiO_2$	148
Au/TiO_2	15	4.7×10^{18}	0.056	$^aTiO_2$	237

$^aTiO_2$ = CO desorption from TiO_2 adsorption sites.

7.3.1.7 Effect of flow rate

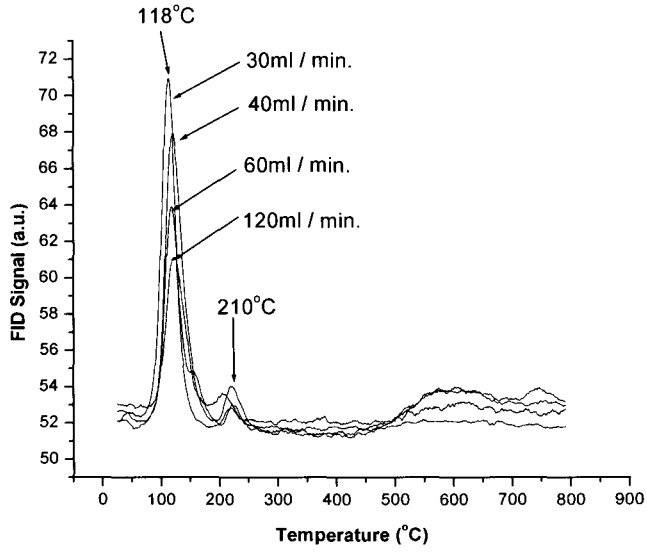


Figure 7.12 Carbon monoxide desorption curves showing effect of the flow rate when 1wt % Au/TiO_2 samples were calcined at 400°C for 1h and carbon monoxide was adsorbed at room temperature and at different flow rates. Desorption was carried out from room temperature to 800°C at 10°C/min. Desorbed CO was detected as methane.

When 1wt% Au/TiO_2 composite material was exposed to carbon monoxide at different flow rates, CO adsorption increased significantly with maximum adsorption obtained at 30 ml/min. At flow rates above 30 ml/min, the amount of the desorbing component decreased. The volume of the desorbing carbon oxide is lower at higher flow rates and the shape of the desorption curve does not change with the flow rate, but the volume of the desorbing component changes. When carbon monoxide is introduced to Au/TiO_2 surface at high flow rates, the surface does not get enough time to adsorb enough molecules of CO, hence the volume of the desorbing carbon monoxide is lower at higher flow rates. The flow rate of the adsorbate (CO or CO_2) used in this work is 30 ml/min.

Table 7.9 Specific adsorption for 1wt% Au/TiO_2 calcined at 400°C for 1h. Carbon monoxide was adsorbed at room temperature for 30 min. at different flow rates. Desorption was carried out from adsorption temperature (rt) to 800°C at 10°C/min.

Desorption temperature maxima (°C)	Flow rate of CO ml/min.	Specific adsorption (molecules/g)	Volume of CO Adsorbed (ml)	Sites
118	30	4.0×10^{19}	0.48	$^{a}TiO_2$
210	30	5.0×10^{18}	0.06	$^{a}TiO_2$
118	40	3.5×10^{19}	0.42	$^{a}TiO_2$
210	40	4.3×10^{18}	0.052	$^{a}TiO_2$
118	60	3.0×10^{19}	0.36	$^{a}TiO_2$
210	60	4.1×10^{18}	0.05	$^{a}TiO_2$
118	120	1.9×10^{19}	0.23	$^{a}TiO_2$
210	120	4.0×10^{18}	0.048	$^{a}TiO_2$

$^{a}TiO_2$ = CO desorption from TiO_2 adsorption sites.

Table 7.9 shows that the specific adsorption is also affected by the flow rate variation. As the flow rate increases, the number of CO molecules binds to the surface of Au/TiO_2 composite material decreases.

7.3.1.8 Effect of gold loading

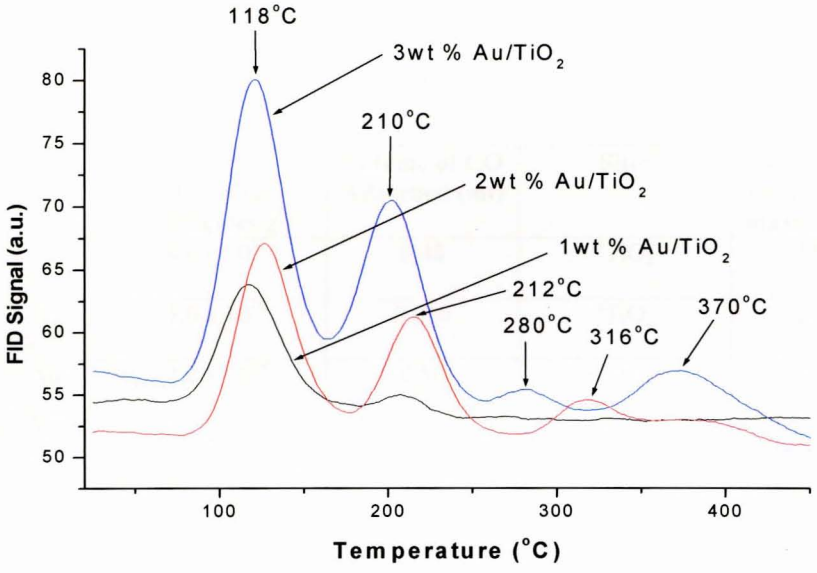


Figure 7.13 Carbon monoxide desorption curves, showing the effect of gold loading. All Au/TiO_2 samples were calcined at 400°C in hydrogen, carbon monoxide was adsorbed at room temperature for 30 min. at 30 ml/min. The desorption process was carried out from room temperature to 500°C at 10°C/min. Desorbed CO was detected as methane.

An increase in gold loading from 1.0 to 2.0 and 3.0 wt% caused an increase in intensity and the number of desorption peaks and consequently influences the number and type of adsorption sites present in the catalyst. Therefore, there is not just simple physical adsorption, gold also influences the number and nature of carbon monoxide adsorption centres on titanium dioxide. As the gold loading increases from 1 to 3 wt%, new active gold sites are observed at 280°C, at 316°C and at 370°C respectively. It seems that increasing the %Au loading leads to chemisorption of CO as indicated in figure 7.13. Further investigations should be done involving E_{ad} (activation energy of adsorption) calculations for catalysts with higher gold loading using the correct desorption peaks.

Table 7.10 Specific adsorption for Au/TiO_2 loaded with different gold concentration. Au/TiO_2 samples were calcined at 400°C for 1h. Carbon monoxide was adsorbed at room temperature for 30 min. at 30 ml/min. Desorption was carried out from room temperature to 500°C at 10°C/min.

Sample	Specific adsorption (molecules/g)	Volume of CO Adsorbed (ml)	Sites	Desorption temperature maxima (°C)
1 wt% Au / TiO_2	4.0×10^{19}	0.48	[a]TiO_2	118
1 wt% Au / TiO_2	5.0×10^{18}	0.060	[a]TiO_2	210
2 wt% Au / TiO_2	4.2×10^{19}	0.50	[a]TiO_2	118
2 wt% Au / TiO_2	2.4×10^{19}	0.29	[a]TiO_2	212
2 wt% Au / TiO_2	4.9×10^{18}	0.058	[b]Au	316
2 wt% Au / TiO_2	5.3×10^{18}	0.063	[b]Au	390
3 wt% Au / TiO_2	5.9×10^{19}	0.71	[a]TiO_2	118
3 wt% Au / TiO_2	3.8×10^{19}	0.45	[a]TiO_2	210
3 wt% Au / TiO_2	5.0×10^{18}	0.060	[b]Au	280
3 wt% Au / TiO_2	1.9×10^{19}	0.23	[b]Au	370

[a]TiO_2 = CO desorption from TiO_2 adsorption sites.

[b]Au = CO desorption from gold particles.

7.3.1.9 Effect of calcination temperature

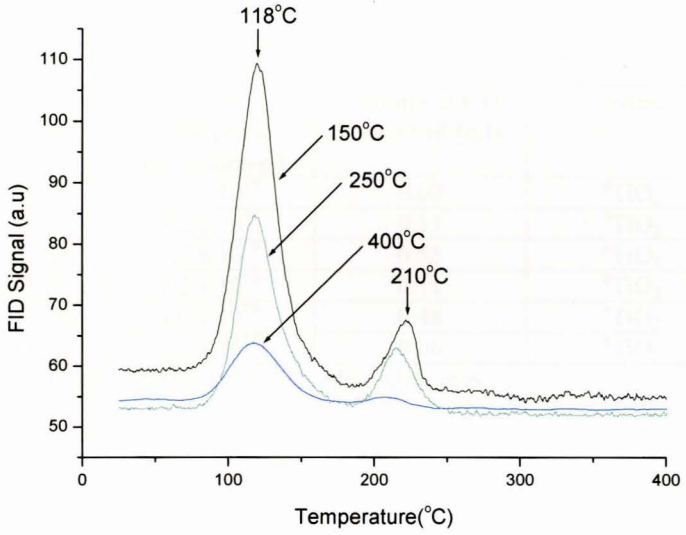


Figure 7.14 Carbon monoxide desorption curves from 1wt% Au/TiO_2 showing the effect of calcination temperature. 1wt% Au/TiO_2 samples were calcined at different temperatures (150°C, 250°C and 400°C) in hydrogen, carbon monoxide was adsorbed at room temperature for 30 min. Desorption was carried out at 10°C/min. from room temperature to 400°C. Desorbed CO was detected as methane.

Effect of calcination temperature on 1wt% Au/TiO_2 composite materials was studied, it was discovered that gold agglomerates at higher temperatures. This was investigated by a decrease in volume of CO adsorbed on these materials after being calcined at higher temperatures.

Table 7.11 Specific adsorption of 1wt% Au/TiO_2 calcined at different temperatures. Carbon monoxide was adsorbed at room temperature for 30min. at 30ml/min. Desorption was carried out at 10°C/min. from room temperature to calcination temperature (150°C, 250°C or 400°C).

Sample	Specific adsorption (molecules/g)	Volume of CO Adsorbed (ml)	Sites	Calcination Temperature (° C)	Desorption temperature maxima (°C)
Au/TiO_2	5.0×10^{19}	0.60	$^{a}TiO_2$	150	118
Au/TiO_2	9.2×10^{18}	0.11	$^{a}TiO_2$	150	210
Au/TiO_2	4.5×10^{19}	0.55	$^{a}TiO_2$	250	118
Au/TiO_2	9.2×10^{18}	0.11	$^{a}TiO_2$	250	210
Au/TiO_2	4.0×10^{19}	0.48	$^{a}TiO_2$	400	118
Au/TiO_2	5.0×10^{18}	0.06	$^{a}TiO_2$	400	210

$^{a}TiO_2$ = CO desorption from TiO_2 adsorption sites.

7.3.2 ADSORPTION OF CARBON DIOXIDE ON TiO_2 OR Au/TiO_2

7.3.2.1 Effect of gold on support (TiO_2) when CO_2 is adsorbed at -80°C

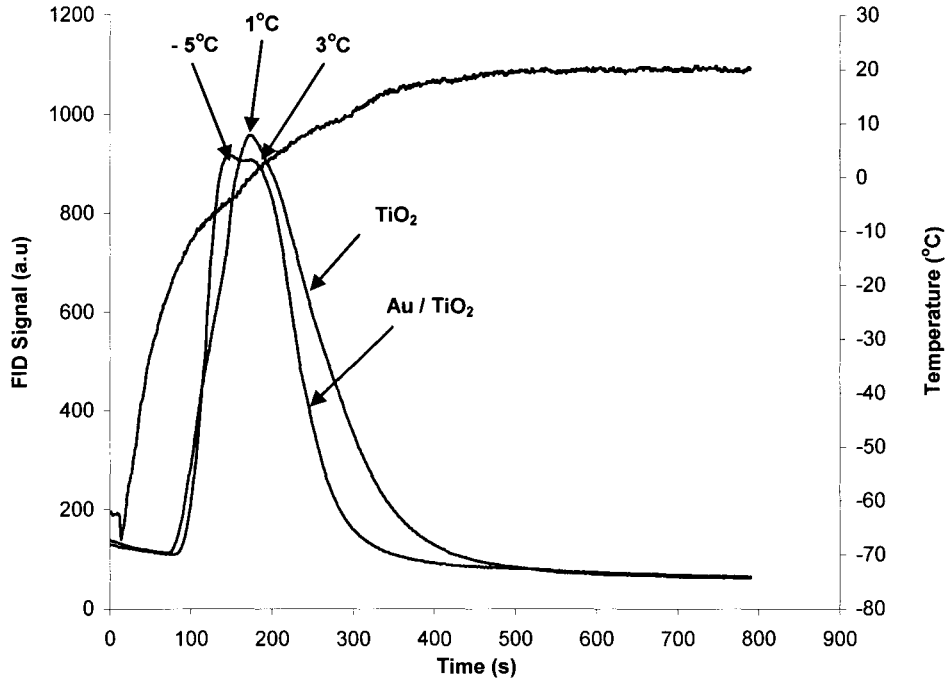


Figure 7.15 Shows the difference between the desorption of carbon dioxide when the sample is changed from TiO_2 to 1wt% Au/TiO_2. 1wt% Au/TiO_2 and TiO_2 were both calcined at 400°C for 1h in hydrogen. Carbon dioxide was adsorbed at -80°C for 30 min. at 30 ml/min. Desorption was carried out from -80°C to room temperature. Desorbed CO_2 was detected as methane.

Figure 7.15 shows the difference between the desorption experiments of carbon dioxide when the sample is changed from TiO_2 to Au/TiO_2. The total volume of CO_2 desorption from the support alone is 17 ml whereas the one obtained from Au/TiO_2 is 13.9 ml from the same type of adsorption sites. The TPD curve of TiO_2 support exhibits very large CO_2 desorption peak with a desorption temperature maximum of 1°C. A single carbon dioxide desorption peak with a doublet is observed on 1wt% Au/TiO_2 sample (figure

7.15), one due to carbon dioxide desorption from the support and the second peak corresponds to carbon dioxide desorption from the perimeter gold sites.

Table 7.12 Specific adsorption for 1wt% Au/TiO_2 and TiO_2 calcined at 400°C for 1h. Carbon dioxide was adsorbed at -80°C for 30 min. at 30 ml/min. Desorption was carried out from -80°C to room temperature.

Sample	Specific adsorption (molecules/g)	Volume of CO_2 Adsorbed (ml)	Catalyst (type of adsorption sites)	Desorption temperature maxima (°C)
TiO_2	1.4×10^{21}	17.0	[a]TiO_2	1
Au/TiO_2	1.1×10^{21}	13.9	[a]TiO_2	-5
Au/TiO_2	1.1×10^{21}	13.5	[b]Au/TiO_2	3

[a]TiO_2 = CO_2 desorption from TiO_2 adsorption sites.

[b]Au/TiO_2 = CO_2 desorption assumed to be from gold sites which are exposed at the contact perimeter between gold particles and the oxide support.

7.3.2.2 Effect of gold on support (TiO_2) when CO_2 is adsorbed at room temperature

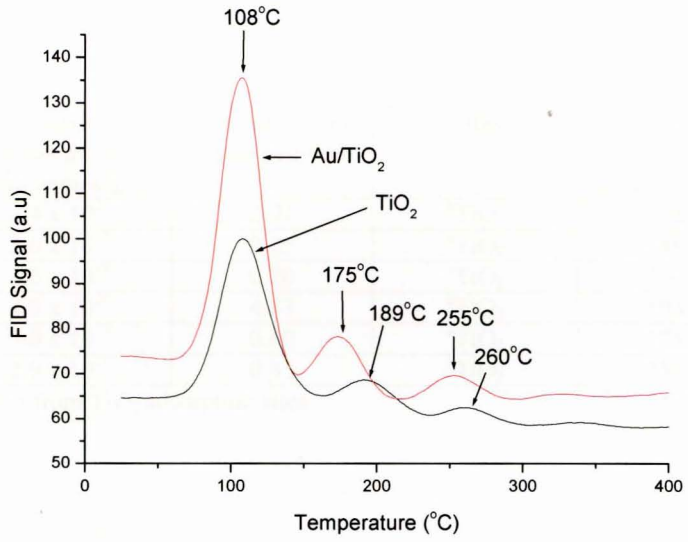


Figure 7.16 Carbon dioxide desorption curves from TiO_2 and 1wt% Au/TiO_2, the catalyst samples were calcined at 400°C for 1h in hydrogen and carbon dioxide was adsorbed at room temperature for 30 min. at 30 ml/min. Desorption was carried out from room temperature to 400°C at 10°C/min. Desorbed CO_2 was detected as methane.

When carbon dioxide was adsorbed on 1wt% Au/TiO_2, three desorption peaks continuing to higher temperatures were observed with desorption temperature maxima of 108°C, 175°C and 255°C respectively. The adsorbed carbon dioxide desorbs as three distinct peaks from both TiO_2 and Au/TiO_2. From carbon dioxide desorption curves (figure 7.16), it is shown that gold increases the amount of the desorbing component from the support (TiO_2). There is no desorption peak attributed to gold but specific adsorption (molecules/g) increases (Table 7.13). This was observed with carbon monoxide as well (figure 7.7).

Table 7.13 Specific adsorption for 1wt% Au/TiO_2 and TiO_2 calcined at 400°C for 1h. Carbon dioxide was adsorbed at room temperature for 30 min. at 30 ml/min. Desorption was carried out from room temperature to 400°C at 10°C/min.

Sample	Specific adsorption (molecules/g)	Volume of CO_2 Adsorbed (ml)	Sites	Desorption temperature maxima (°C)
TiO_2	2.4×10^{20}	2.91	$^aTiO_2$	108
TiO_2	2.0×10^{19}	0.25	$^aTiO_2$	189
TiO_2	1.6×10^{19}	0.20	$^aTiO_2$	260
Au/TiO_2	4.0×10^{20}	4.83	$^aTiO_2$	108
Au/TiO_2	5.0×10^{19}	0.60	$^aTiO_2$	175
Au/TiO_2	2.9×10^{19}	0.35	$^aTiO_2$	255

$^aTiO_2$ = CO_2 desorption from TiO_2 adsorption sites.

7.3.2.3 Effect of heating rate

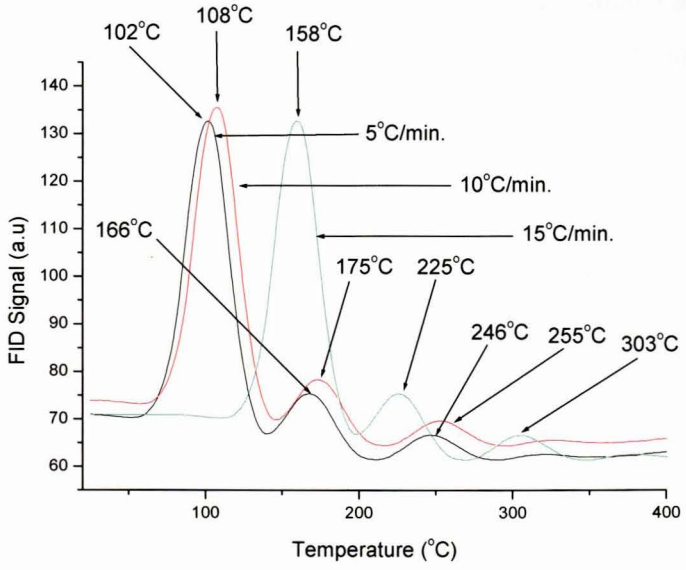


Figure 7.17 Carbon dioxide desorption curves. Carbon dioxide was adsorbed at room temperature for 30 min. at 30 ml/min. 1wt% Au/TiO_2 samples were calcined at 400°C for 1h in hydrogen. Desorption occurred from room temperature to 400°C at different heating rates.

From the slope of the line, activation energy of 6.0 kJ/mol is obtained (figure 7.18). This shows that carbon dioxide is weakly bound on the surface of Au/TiO_2 composite material similar to the situation with carbon monoxide.

There is a possibility that carbon monoxide desorbs as carbon dioxide as revealed by identical activation energy of desorption for both CO and CO_2. Further work with mass spectrometry analysis is required to prove this.

The heating rate variation was found to have a significant effect on TPD experiments. As the heating rate increased the desorption peaks shifted towards high temperatures as shown in figure 7.17. As the heating rate increases, the higher thermal agitation between the molecules occurs and that affects the rate of desorption of carbon dioxide from 1wt% Au/TiO_2 composite material. The volume and the shape of the desorption peaks are not affected by the heating rate variation, but the position of the peak (peak temperature) is. From these results, the activation energy of desorption was calculated and obtained to be 6.0 kJ/mol. This suggests that carbon dioxide is physisorbed on 1wt% Au/TiO_2 composite material.

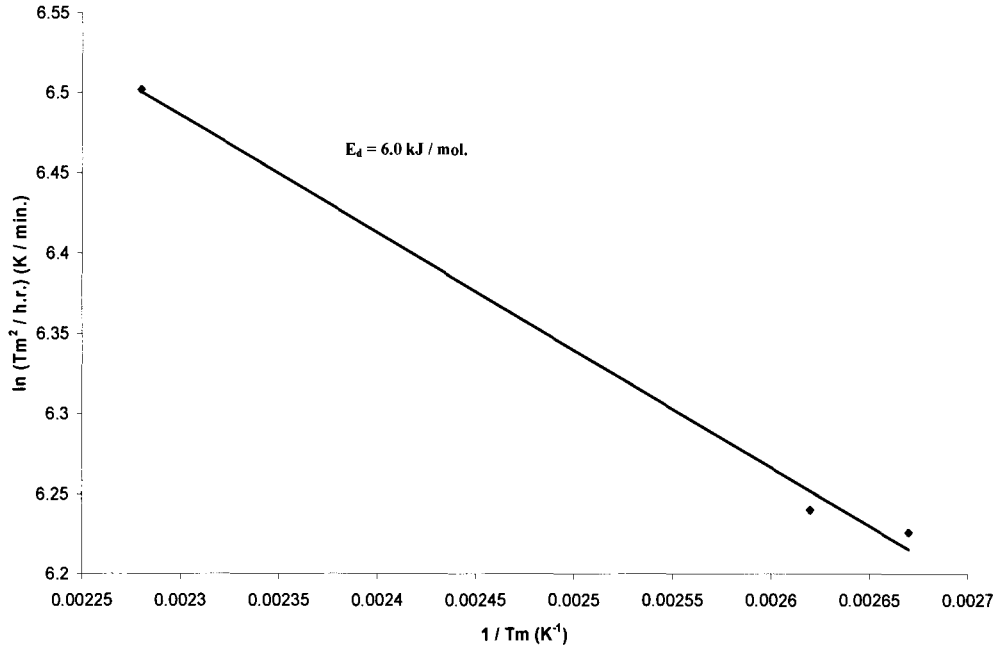


Figure 7.18 Activation energy determination from heating rate variation, ln (Tm^2/h.r.) against $1/T_m$ (K^{-1}) for carbon dioxide.

Table 7.14 Specific adsorption for 1wt% Au/TiO_2 calcined at 400°C for 1h. Carbon dioxide was adsorbed at room temperature for 30 min. at 30 ml/min. Desorption was carried out from room temperature to 400°C at different heating rates.

Sample	Heating rate °C/min.	Specific adsorption (molecules/g)	Volume of CO_2 Adsorbed (ml)	Sites	Desorption temperature maxima (°C)
Au/TiO_2	5	4.0×10^{20}	4.83	$^aTiO_2$	102
Au/TiO_2	5	5.0×10^{19}	0.60	$^aTiO_2$	166
Au/TiO_2	5	2.9×10^{19}	0.35	$^aTiO_2$	246
Au/TiO_2	10	4.0×10^{20}	4.83	$^aTiO_2$	108
Au/TiO_2	10	5.0×10^{19}	0.59	$^aTiO_2$	175
Au/TiO_2	10	2.9×10^{19}	0.35	$^aTiO_2$	255
Au/TiO_2	15	4.0×10^{20}	4.84	$^aTiO_2$	158
Au/TiO_2	15	5.0×10^{19}	0.61	$^aTiO_2$	225
Au/TiO_2	15	2.8×10^{19}	0.34	$^aTiO_2$	303

$^aTiO_2$ = CO_2 desorption from TiO_2 adsorption sites.

7.3.2.4 Adsorption of CO or CO_2 on 1wt% Au/TiO_2

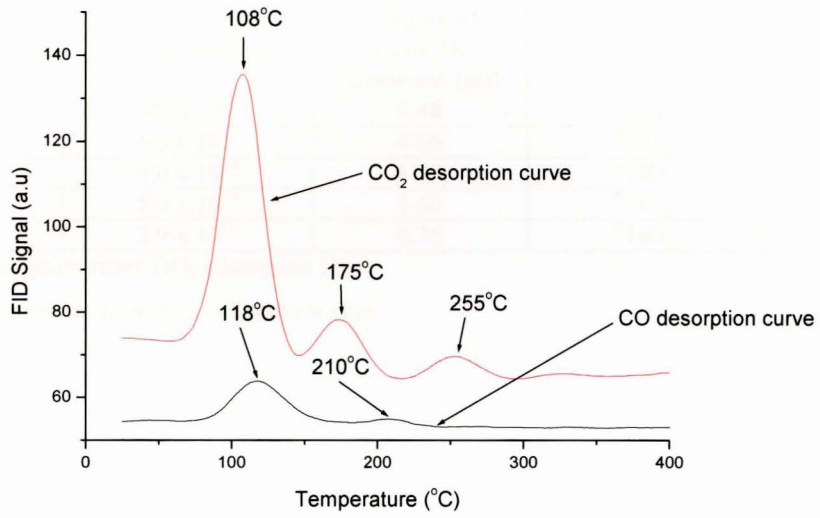


Figure 7.19 Carbon monoxide and carbon dioxide desorption curves from 1wt% Au/TiO_2. Carbon monoxide or carbon dioxide was adsorbed at room temperature for 30 min. at the flow rate of 30 ml/min. 1wt% Au/TiO_2 samples were calcined at 400°C for 1h. Desorption was carried out from room temperature to 400°C at a heating rate of 10°C/min. Both carbon oxides desorbed were detected as methane.

The shape of the desorption curves for both carbon dioxide and carbon monoxide looks identical, there is not much difference in peak position too. The amount of carbon dioxide desorbing from 1wt% Au/TiO_2 is more than the amount of carbon monoxide desorbing from the same material. This may be due to the fact that carbon monoxide used in this work was only 10% and the balance was helium whereas CO_2 was 99.9%. Carbon dioxide and carbon monoxide physisorb on Au/TiO_2 composite material (figure 7.11 and 7.18). Because the activation energies of desorption for both carbon monoxide and carbon dioxide is similar (6.0 kJ/mol.), gold oxidizes carbon monoxide to carbon dioxide.

Table 7.15 Specific adsorption for 1wt % Au/TiO_2 calcined at 400°C in hydrogen for 1h. Carbon monoxide and carbon dioxide were adsorbed at room temperature for 30 min. at 30 ml/min. Desorption was carried out from room temperature to 400°C at 10°C/min.

Adsorbate	Specific adsorption (molecules/g)	Volume of CO/CO_2 Adsorbed (ml)	Sites	Desorption temperature maxima (°C)
CO	4.0×10^{19}	0.48	$^{a}TiO_2$	118
CO	5.0×10^{18}	0.06	$^{a}TiO_2$	210
CO_2	4.0×10^{20}	4.83	$^{b}TiO_2$	108
CO_2	5.0×10^{19}	0.60	$^{b}TiO_2$	175
CO_2	2.9×10^{19}	0.35	$^{b}TiO_2$	255

$^{a}TiO_2$ = CO desorption from TiO_2 adsorption sites.

$^{b}TiO_2$ = CO_2 desorption from TiO_2 adsorption sites.

7.4 POWDER X - RAY DIFFRACTION (PXRD)

7.4.1 EFFECT OF GOLD ON ANATASE-RUTILE PHASE TRANSFORMATION

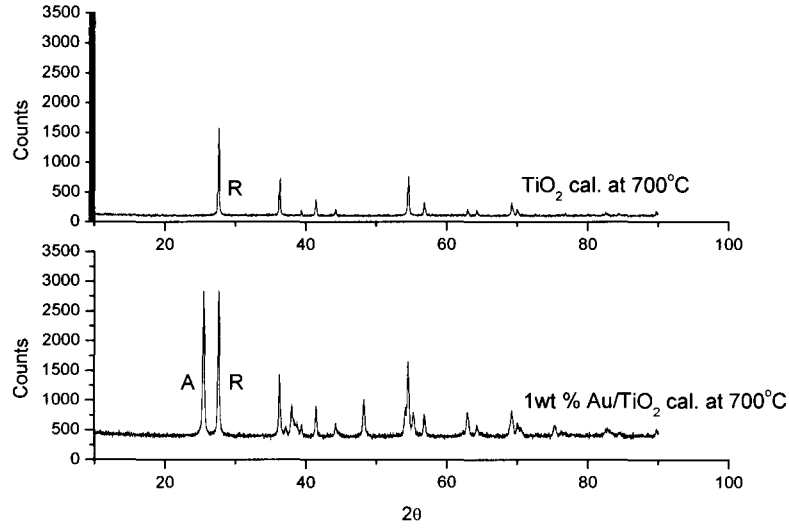


Figure 7.20 Powder X-Ray Diffraction patterns of 1wt% Au/TiO_2 and TiO_2 showing the effect of gold on anatase - rutile phase transformation. All samples were calcined at 700°C for 5hrs. A = anatase and R = rutile

Several elements have been used as dopants that retard or accelerate this anatase – rutile phase transition [3]. There is a general agreement in the literature that the dopants that increase a high concentration of oxygen vacancies in TiO_2 will accelerate the anatase to rutile phase transition whereas dopants that reduce such vacancies will stabilise the anatase phase [4]. Copper has been known to accelerate the anatase to rutile phase transformation [5, 6], gold has been reported to delay it [7]. Powder X-Ray Diffraction results investigate that a little amount of gold (1wt% Au) deposited on titanium dioxide support inhibits the anatase – rutile phase transformation as evidenced in figure 7.20.

When titanium dioxide was calcined at 700°C, nearly all anatase particles were transformed to the rutile phase. 1wt% Au/TiO_2 diffraction pattern shows that the material after calcination at 700°C is still constituted with 50% anatase and 50% rutile. Gold inhibits the anatase - rutile phase transition [7].

The total number of gold perimeter sites was calculated from the average gold particle size and the gold loading and found to be 1 x 10^{18}/g for 1wt% Au/TiO_2. This figure is close to the minor contribution to adsorption on 1wt% Au/TiO_2 measured as 4.9 x 10^{18} (figure 7.1, peak with the desorption temperature maximum of 10°C).

6.5 REFERENCES

[1] K. Mallick, M.S. Scurrell, Appl. Catal. A **253** (2003) 527.

[2] J.M. Gottfried, K.J. Schmidt, S.L.M. Schroeder, K. Christmann, Surf. Sci. **536** (2003) 206.

[3] F. C. Gennari, D.M. Pasquevich, J. Am. Ceram. Soc. **82** (1999) 1915.

[4] R. Arroyo, G. Cordoba, J. Padilla, V. H. Lara, Mater. Lett. **54** (2002) 397.

[5] J. Nair, P. Nair, F. Mizukami, Y. Oosawa, T. Okuba, Mater. Res. Bull. **34** (1999) 1275.

[6] C. Langlade, B. Vannes, T. Sarnet, M. Autric, Appl. Surf. Sci. **186** (2002) 145.

[7] A. G. Shastri, A.K. Datye, J. Schwank, J. Catal. **87** (1984) 265.

CHAPTER 8

CONCLUSIONS AND FUTURE WORK

Titania as one of the best and most used supports for gold deposition since it is possible to obtain a high dispersion of the gold phase producing very active catalysts. Gold supported on titanium dioxide has been used in this work, to study the effect of gold on the surface properties of titanium dioxide. The catalysts were characterized by temperature-programmed desorption (TPD) and Powder X-Ray Diffraction to see the effect of gold on the structural properties of titanium dioxide and to attempt to characterize any crystalline gold present. Both carbon monoxide and carbon dioxide were adsorbed on the surface of these materials at room temperature or at -80°C. Carbon monoxide desorbs as two peaks from titanium dioxide. Its desorption temperature maxima from titanium dioxide are 118°C and 210°C respectively. 1wt% gold deposited on titanium dioxide increased the amount of the desorbing component from the support (TiO_2). There is no desorption peak attributed to gold but specific adsorption (molecules/g) increased due to gold.

Activation energy of desorption was calculated from the desorption results and was found to be 6.0 kJ/mol for both CO and CO_2. This low value of activation energy indicates that CO and CO_2 are weakly adsorbed on 1wt% Au/TiO_2 solid material. The total volume of the adsorbate did not change that much with heating rate but the peak position did.

Therefore carbon monoxide desorbs as carbon dioxide from 1wt% Au/TiO_2 as revealed by identical activation energy of desorption for both carbon oxides. Further work with mass spectrometry analysis is required to prove this.

Also, carbon monoxide desorption curve is very similar to carbon dioxide one, suggesting that CO is oxidized to CO_2 on 1wt% Au/TiO_2 composite materials, even in the absence of dioxygen. Therefore gold oxidizes carbon monoxide to carbon dioxide.

An increase in gold loading from 1.0 to 2.0 and 3.0 wt% caused an increase in peak intensity, in the number of desorption peaks and consequently influenced the number and type of adsorption sites present in the catalyst.

The effect of the flow rate variation was studied on the desorption curves and the results showed that the amount of the desorbing component is lower at higher flow rates.

The specific adsorption was also calculated from the desorption results, there is many number of CO or CO_2 molecules bound to the surface of these materials at low temperatures (when both these carbon oxides are adsorbed at -80°C and the desorption carried out from -80°C to room temperature) than at higher temperatures (when both these carbon oxides are adsorbed at room temperature and the desorption done from room temperature to 800°C at 10°C/min.).

The total number of gold perimeter sites was calculated from the average gold particle size and the gold loading and was found to be 1×10^{18} /g for 1wt% Au/TiO_2. This figure is close to the minor contribution to adsorption on 1wt% Au/TiO_2 measured as 4.9×10^{18}.

8.1 FUTURE WORK

Future research work that may be developed out of this study could involve the following:

- Adsorption of carbon monoxide or carbon dioxide on gold supported on titanium dioxide samples when the samples are calcined at low temperatures (100°C to 200°C) to study the effect of gold on the surface properties of titanium dioxide.

When gold/titanium dioxide samples are calcined at higher temperatures, gold agglomerates and this can affect the behaviour of gold on desorption of CO or CO_2.

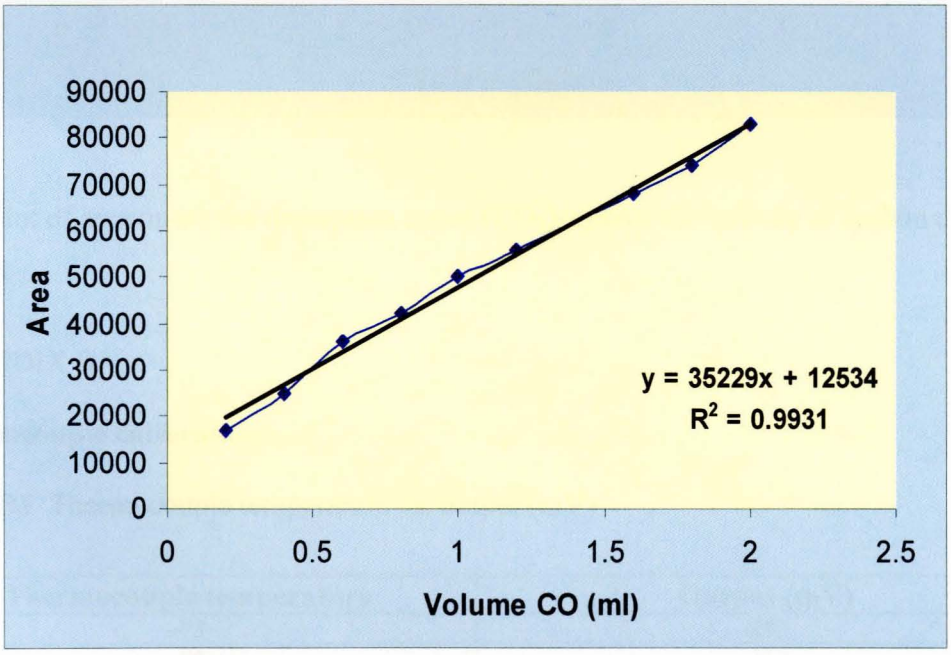
- Adsorption / desorption of carbon monoxide or carbon dioxide on these solid materials with the mass spectrometry attached to the TPD system to identify the types of gas desorbing from the surface of these solids.
- Chemisorption studies on Au/TiO_2

APPENDICES

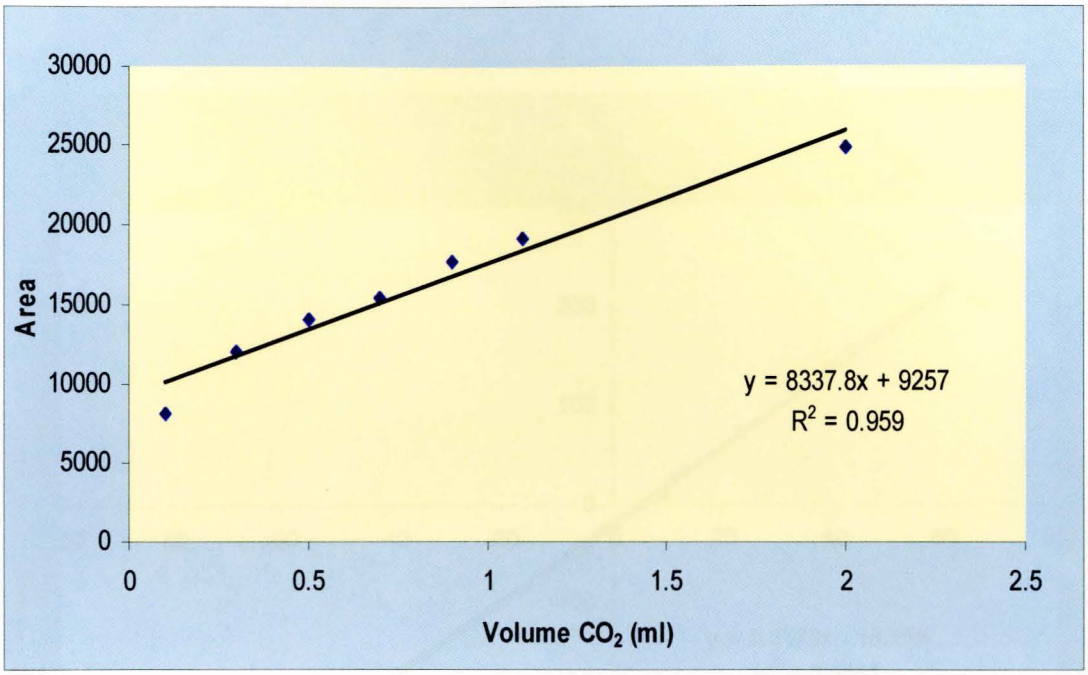
APPENDIX A

Carbon monoxide or carbon dioxide calibration

Calibration of carbon monoxide or carbon dioxide was done by injecting known CO or CO_2 volumes into an empty reactor with flowing helium using a syringe. Area was determined from the desorption curves and a plot of area under the curve against the volume of the adsorbate (CO/CO_2) was drawn and the graph was a straight line.



A1 A plot of area under the desorption curve (CO) against the volume of carbon monoxide.



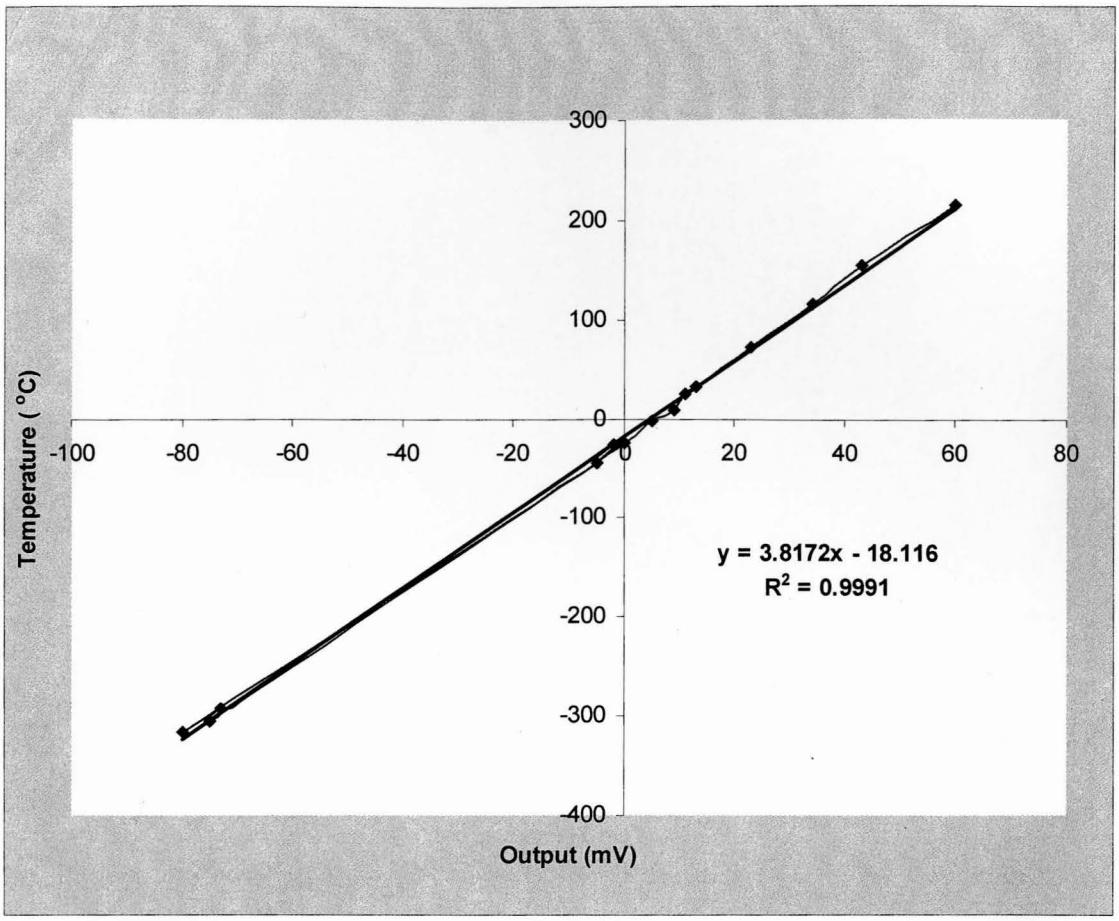
A2 A plot of area under the desorption curve (CO_2) against the volume of carbon dioxide.

APPENDIX B

Thermocouple calibration

Table B1 Thermocouple temperature vs. output (mV)

Thermocouple temperature	Output (mV)
-73	-293
-80	-317
-5	-45
-2	-27
-75	-306
0	-25
5	-2
9	8
11	24
13	32
23	72
34	115
43	154



B2 Thermocouple temperature (^{o}C) vs Output (mV)